

MOBILITY REDUCTION OF CO₂ USING CO₂ SOLUBLE SURFACTANTS

by

William James McLendon

BS in Chemistry, University of Arizona, 2004

Submitted to the Graduate Faculty of
Swanson School of Engineering in partial fulfillment
of the requirements for the degree of
Master of Science

University of Pittsburgh

2012

UNIVERSITY OF PITTSBURGH
SWANSON SCHOOL OF ENGINEERING

This thesis was presented

by

William James McLendon

It was defended on

July 24th, 2012

and approved by

Erick J. Beckman, PhD, Professor, Department of Chemical and Petroleum Engineering

Stephen R. Little, PhD, Chair of the Department of Chemical and Petroleum Engineering

Thesis Advisor: Robert M. Enick, PhD, Professor, Department of Chemical and Petroleum Engineering

MOBILITY REDUCTION OF CO₂ USING CO₂ SOLUBLE SURFACTANTS

William J. McLendon, MS

University of Pittsburgh, 2012

Addition of slightly CO₂-soluble, brine-soluble, surfactants to high pressure CO₂ for EOR may facilitate in-situ generation of CO₂-in-brine foams for mobility control. These non-ionic surfactants have been demonstrated to dissolve in CO₂ to concentrations of 0.1wt% at reservoir conditions and stabilize CO₂-in-brine foams in a high pressure windowed cell. One such surfactant is Huntsman SURFONIC[®] N, a branched nonylphenol ethoxylates with averages of 12 (N-120) or 15(N-150) ethylene oxide repeat units in the hydrophile. SURFONIC[®] N-120 was selected for mobility reduction studies involving flow of CO₂ into brine-saturated porous media.

Transient mobility measurements were conducted using a water-wet Berea core (104mD), water-wet Bentheimer sandstone core (~1500mD), and several SACROC carbonate cores (3.6 and 8.9mD). The CO₂ was injected into brine-saturated cores at superficial velocity of 10 ft/day, and surfactant was either not used (control), dissolved only in brine at 0.07wt%, dissolved only in CO₂ at ~0.07wt%, or dissolved in brine and CO₂ at 0.07wt%. In general, in-situ foam generation in relatively high permeability sandstone was evidenced during the first few pore volumes of CO₂ injected by pressure drops that were 2-3 times greater than control tests regardless of what phase CO₂ was in. Mobility reduction was more modest (20–50% increases in pressure drop) in lower permeability SACROC cores (3.6 and 8.9mD) when surfactant was dissolved in CO₂. With surfactant dissolved in brine, pressure drops increased by a factor of 2–3 when CO₂ was injected into an 8.9mD core.

High pressure CT imaging of in-situ foam generation was conducted by injecting high pressure CO₂ into 5wt% KI-brine-saturated Berea sandstone (3-8mD). Tests with no surfactant (control), or with surfactant dissolved either brine or CO₂ at ~0.07wt%. At lower superficial velocities (0.47ft/day), in-situ foam generation was obvious only when surfactant was dissolved in brine. Higher flow rates (4.7ft/day) preferential flow of CO₂ through high permeability layers and viscous fingering within layers that occurred during control tests was suppressed by addition of surfactant to either CO₂ or brine. The most distinct CO₂ foam front occurred with surfactant dissolved in brine.

TABLE OF CONTENTS

PREFACE	ix
1.0 INTRODUCTION	1
2.0 OBJECTIVE	4
3.0 EXPERIMENTAL	10
3.1 TRANSIENT MOBILITY (PRESSURE DROP) MEASUREMENTS: CO₂ INVADING BRINE-SATURATED BEREA SANDSTONE	10
3.2 CT IMAGING OF CO₂ INVADING BRINE-SATURATED POLYSTYRENE CORE	11
4.0 RESULTS	12
4.1 TRANSIENT MOBILITY MEASUREMENTS	12
4.2 CT IMAGING	18
5.0 CONCLUSIONS	28
BIBLIOGRAPHY	30

LIST OF TABLES

Table 1. Conditions for CT imaging displacements, 23 °C 2200 or 2300 psi, CO ₂ invading a 5wt% KI brine-saturated Berea sandstone core; *permeability values for all cores not measured, those cores were estimated to be ~ 20% porous and ~5 mD	19
---	----

LIST OF FIGURES

Figure 1. Branched nonylphenol ethoxylate.....	4
Figure 2. The solubility of SURFONIC® N-120 and N-150 in CO ₂ at 25 °C.....	5
Figure 3. The solubility of SURFONIC® N-120 and N-150 in CO ₂ at 58.....	5
Figure 4. Foam stability associated with Huntsman SURFONIC® N-120 and N-150 surfactants at 1300 psia and 25 °C.....	6
Figure 5. Pressure drop across a 6” long, 1” diameter, 104 md Berea sandstone core.....	7
Figure 6a. CT slices of CO ₂ within PS cores (~30 mD), ~2700 psi and 23°C.....	8
Figure 6b. Mean Computed Tomography Number (CTN) along the length of the 6” PS core.....	9
Figure 7a. Displacement of brine, either 5wt% NaCl or SACROC brine, with CO ₂ at 21°C, 2700 psi. Bentheimer sandstone core (25% porosity, 1550 mD, 2.03” length, 1” diameter). CO ₂ injection rate 1mL/min, 10 ft/day.....	13
Figures 7b. Displacement of brine, either 5wt% NaCl or SACROC brine, with CO ₂ at 21°C, 2700 psi. Bentheimer sandstone core (25% porosity, 1550 mD, 2.03” length, 1” diameter). CO ₂ injection rate 1mL/min, 10 ft/day.....	14
Figure 8. Displacement of SACROC brine with CO ₂ at 21°C, 2700psi.....	15
Figure 9. Displacement of SACROC brine (6.6wt% NaCl, 1.2wt% CaCl ₂ , 0.4wt% MgCl ₂) with CO ₂ at 21°C, 2700 psi. SACROC carbonate core (8.9mD, porosity 16.5 %, 2.6” length, 1” diameter).....	16
Figure 10. Displacement of 5wt% NaCl brine with CO ₂ at 21°C, 2700 psi. SACROC carbonate core (3.6mD, porosity 14% porosity, 2” length, 1” diameter). Superficial velocity of 10 ft/day. Control tests with no surfactant, and a test with surfactant in CO ₂	17
Figure 11: Low flow rate test (0.2 ml/min, 0.47 ft/day) in low permeability Berea sandstone (4.7 mD) control....	20
Figure 12: Low flow rate test (0.2 ml/min, 0.47 ft/day) in low permeability Berea sandstone (3.2 mD); surfactant N-150 in brine.....	21

LIST OF FIGURES

Figure 13. Low flow rate test (0.2 ml/min, 0.47 ft/day) in low permeability Berea sandstone (3.0 mD); surfactant N-150 in CO ₂	22
Figure 14. High flow rate test (2.0 ml/min, 4.7 ft/day) in low permeability Berea sandstone (6.0 mD); control test.....	23
Figure 15. High flow rate test (2.0 ml/min, 4.7 ft/day) in low permeability Berea sandstone (5.0 mD); Surfactant N-120 in brine.....	24
Figure 16. High flow rate test (2.0 ml/min, 4.7 ft/day) in low permeability Berea sandstone (3.9 mD); surfactant N-150 in brine.....	25
Figure 17. High flow rate test (2.0 ml/min, 4.7 ft/day) in low permeability Berea sandstone (7.6 mD); surfactant N-120 in CO ₂	26
Figure 18. High flow rate test (2.0 ml/min, 4.7 ft/day) in low permeability Berea sandstone (6.1 mD); surfactant N-120 in CO ₂	27

PREFACE

I would like to thank first and foremost Dr. Robert M. Enick, who gave me the opportunity and helped drive me to achieve success. A special thanks to Dr. T.R. McLendon whose guidance and tutelage have helped me get through this research and through life. Further, a special thanks for Huntsman for supporting the post-doctoral work of Peter Koronaios and providing the surfactant samples and also Kinder Morgan for providing us with SACROC cores, crude oil, and produced brine samples. I also appreciate the generous financial support of this research project provided by the US DOE via the National Energy Technology Laboratory's Regional University Alliance, NETL RUA. This technical effort was performed in support of the National Energy Technology Laboratory's on-going research in "Novel Surfactant-Based Concepts for Improved Mobility Control of CO₂ Floods" under RES contract DE-FE0004000.4.650.920.001. I would like to acknowledge the technical contributions of Bryan Tennant (CT imaging).

1.0 INTRODUCTION

Mobility control during CO₂ floods is typically realized using the water-alternating-gas process (WAG), while various types of gels can be employed to block thief zones. A recent literature review (Enick and Olsen, 2011) indicates that there have been extensive studies of chemically-based techniques for the near-wellbore diversion of CO₂ from watered-out zones and/or improving in-depth mobility control throughout the formation. The most notable concept is the in-situ generation of CO₂-in-brine foams via the alternating injection of aqueous surfactant solutions and CO₂ gas (SAG). Numerous laboratory studies and about a dozen pilot-scale tests indicated that these foams were used primarily for either near-wellbore conformance control in lateyed formations by generating strong foam in watered-out zones, or (in fewer cases) for in-depth mobility control by generating weaker foam that would inhibit fingering in the oil-bearing zone (Enick and Olsen 2011). To some degree, both conformance control and mobility control could be accomplished with SAG.

In an attempt to provide operators with an additional option for generating foams in-situ, surfactant can be dissolved in CO₂ rather than brine. The injection of a CO₂-surfactant solution would ensure that the surfactant would be available for foam generation in the porous medium wherever the CO₂ was flowing, rather than depending on CO₂ flowing into the same portions of the formation invaded by a previously injected aqueous surfactant solution during SAG. The CO₂-surfactant solution would also be capable of generating foam with in-situ brine, possibly reducing or even eliminating the need for alternating injections of brine; this would be of particular interest to operators that only employ continuous CO₂ to recover oil. The identification of CO₂-soluble foaming surfactants would also enable one to conduct an in-situ foam generation mobility control process in which surfactant was present in the alternating CO₂ and brine slugs, thereby enhancing the likelihood that foams would form in-situ.

The notion of dissolving a surfactant into CO₂ during an enhanced oil recovery process for the purpose of generating CO₂-in-brine mobility control foam or conformance control foam was suggested by Bernard and Holm in their 1967 patent (Bernard and Holm 1967), but data validating the solubility of surfactants in CO₂ was not provided. Dense CO₂ is indeed a feeble solvent for compounds with polar segments, and the identification of surfactants that could dissolve at appreciable concentrations in CO₂ and stabilize CO₂-in-brine foams is a

challenging design problem. The CO₂-insolubility of most surfactants, particularly ionic surfactants, was addressed by Irani's patent ([Irani et al. 1989](#)). Irani suggested that a co-solvent should be added to the CO₂ in an attempt to dissolve siloxane-based surfactants, which – like CO₂ – have very low solubility parameters ([Irani 1989](#)). In 1991, Schievelbein's patent suggested that a co-solvent could be avoided if non-ionic hydrocarbon-based surfactants were considered. Schievelbein recommended using at least 0.2wt% (2000 ppm) of an ethoxylated alkyl or ethoxylated alkyl aryl (i.e. alkyl phenol) hydrocarbons that contain an alkyl chain with an average of 7 to 15 carbons and an average of between 1 to 7 ethoxide (i.e. ethylene oxide or EO) units ([Schievelbein 1991](#)). Typically, surfactants with such short EO tails are likely to be brine-insoluble or brine-dispersible. This lack of solubility in the aqueous phase makes such surfactants unlikely stabilize CO₂-in-brine foams, which are readily formed when the surfactant is more soluble in the aqueous phase than in the dense CO₂.

There has been a great deal of renewed interest in CO₂-soluble surfactants for both petroleum and chemical engineering applications during the last decade. As a result, commercially available, brine-soluble, non-ionic surfactants have been identified that are not only slightly soluble in CO₂ (e.g. several tenths of a weight percent), but also capable of stabilizing CO₂-in-brine foams. Johnston and coworkers ([Dhanuka et al. 2006](#)) noted that Dow Tergitol TMN surfactants were CO₂-soluble ([Ryoo 2003](#)) and that TMN 6 (Mw = 552) poly(ethylene glycol)_{8,33} 2,6,8-trimethyl-4-nonyl ether (90% active, 10% water) was an effective foaming agent. Johnston and co-workers also investigated the ability of di-block and tri-block surfactants with siloxane-based, fluorocarbon-based and polyalkyloxide-based CO₂-philic segments to stabilize CO₂-in-water emulsions ([daRocha et al. 2001](#)). Our research group established that oligo(vinyl acetate) (OVAc) is extremely CO₂-philic and suitable for incorporation into CO₂-soluble ionic surfactants ([Fan et al. 2005](#)). [Tan and Cooper \(2005\)](#) used polyethylene oxide (PEO) as the hydrophilic during their design of tri-block OVAc-b-PEO-b-OVAc surfactants capable of stabilizing CO₂ foams.

In 2008, researchers from the University of Texas at Austin and Dow Oil & Gas used a proprietary non-ionic surfactant at a concentration of ~0.1wt% in CO₂ to recover oil from a core ([Le et al. 2008](#)). They found that the injection of the CO₂-surfactant solution into the waterflooded core without the use of alternating water slugs yielded higher oil recovery than WAGS (water-alternating -gas with surfactant dissolved in the CO₂), and SAG (surfactant-alternating-CO₂ with surfactant dissolved in the water). Recently, the same type of surfactant was tested by Dow Oil & Gas in a SACROC pilot flood operated by Kinder Morgan ([Sanders 2010](#); [Sanders, Jones et al. 2010](#)). The results indicated that a reduction in CO₂ injection at a constant pressure occurred while 30% of the CO₂ was diverted

into zones that had previously not seen CO₂. Both of these trends indicated that reduced-mobility CO₂-in-brine foams had formed in-situ. The University of Texas at Austin and Dow Oil & Gas presented a study of the morphologies, stabilities, and viscosities of high-pressure carbon dioxide-in-water foams formed with water-soluble, branched, nonionic hydrocarbon surfactants that did not contain an aromatic or cyclic functionality (Adkins, Chen, Chan, et al. 2010). The surfactant solubility in dense CO₂ was not presented, however. Foams were formed by dissolving the surfactant in the brine and then co-injecting this aqueous surfactant solution along with high pressure CO₂ into a sand pack with hydrophilic pores. Most of the surfactants did form foams at 24°C, and the surfactants with high cloud point temperatures (for 1wt% aqueous solutions) yielded foams at the highest temperatures. They also described a new, non-ionic, glycerin-based, twin-tailed, water-soluble, ethoxylated surfactant for stabilizing CO₂-in-water emulsions used for CO₂ flooding sweep improvement (Sanders, Nguyen et al. 2010). Johnston and co-workers investigated a biocompatible, water-soluble, nonionic, ethoxylated surfactant, polyoxyethylene (20) sorbitan monooleate (polysorbate 80, Tween 80) for stabilizing CO₂-in-water and water-in-CO₂ emulsions and double-emulsions (Torino et al. 2010).

Recently, NETL and the University of Pittsburgh presented a studied numerous commercially available, inexpensive, non-ionic surfactants that were capable of dissolving in CO₂ in dilute concentration at typical minimum miscibility pressure (MMP) conditions and, upon mixing with brine in a high pressure windowed cell, stabilizing CO₂-in-brine foams (Xing et al. 2010). These slightly CO₂-soluble, water-soluble surfactants include branched alkylphenol ethoxylates, branched alkyl ethoxylates, a fatty acid-based surfactant, and a predominantly linear ethoxylated alcohol. Many of the surfactants were between 0.02 - 0.06wt% soluble in CO₂ at 1500 psia and 25 °C, and most demonstrated some capacity to stabilize foam. The most stable foams were realized with branched alkylphenol ethoxylates, several of which were studied in high pressure small angle neutron scattering (HP SANS) tests. HP SANS analysis of foams residing in a small windowed cell demonstrated that the nonylphenol ethoxylate Huntsman SURFONIC® N-150 (an average of 15 EO groups in the ethoxylate tail) generated foams with a greater concentration of droplets and a broader distribution of droplet sizes than the shorter chain analogues with 9–12 ethoxylates.

2.0 OBJECTIVE

In this work, the efficacy of one of the types of non-ionic surfactants recently assessed by our group, a branched nonylphenol ethoxylate (e.g. Huntsman SURFONIC[®] N-120 and N-150 shown in [Figure 1](#)), is assessed as a CO₂-soluble mobility control additive using transient mobility experiments and CT imaging.

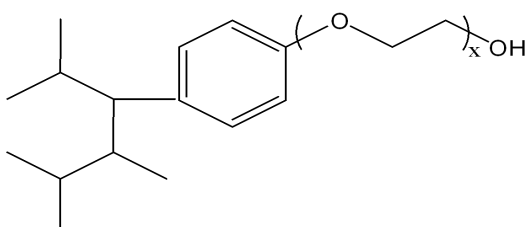


Figure 1. Branched nonylphenol ethoxylate; Huntsman SURFONIC[®] N-120 and N-150, $x_{\text{average}} = 12$ and 15 , respectively. This is a representative alkyl tail; the tails of the commercial surfactant consist of mixed C₉ isomers); The pour points of N-120 and N-150 are 2.8 °C and 17.2 °C, respectively.

We have previously determined the solubility of both surfactants in CO₂ at 25 °C and 58 °C. The results, shown in [Figures 2 and 3](#) ([Xing et al. 2010](#); [Xing et al. 2011](#)), were obtained via a standard non-sampling technique in which the solubility was measured during the very slow expansion of a transparent, single-phase, high pressure mixture of known amounts of CO₂ and the surfactant. The dew point pressure, shown by the markers in [Figures 2 and 3](#), correspond to the pressure value at which a cloud (i.e. very fine mist) of a second phase, a surfactant-rich liquid, first appeared and prevented one from discerning objects behind the 1 inch diameter sample volume.

Both surfactants have also been shown to stabilize CO₂-in-brine foams in agitated, windowed, high pressure phase behavior cells ([Xing et al. 2010](#)). In these experiments equal amounts of brine and dense CO₂ were mixed vigorously along with the amount of surfactant that could be dissolved in the CO₂ at test conditions. After mixing ceased, foam initially filled the entire cell. The rate of collapse of the CO₂-in-brine foam, which was quantified by measuring the rate of appearance of a clear brine phase below the foam and, in some cases, the appearance of a clear CO₂ phase above the foam.

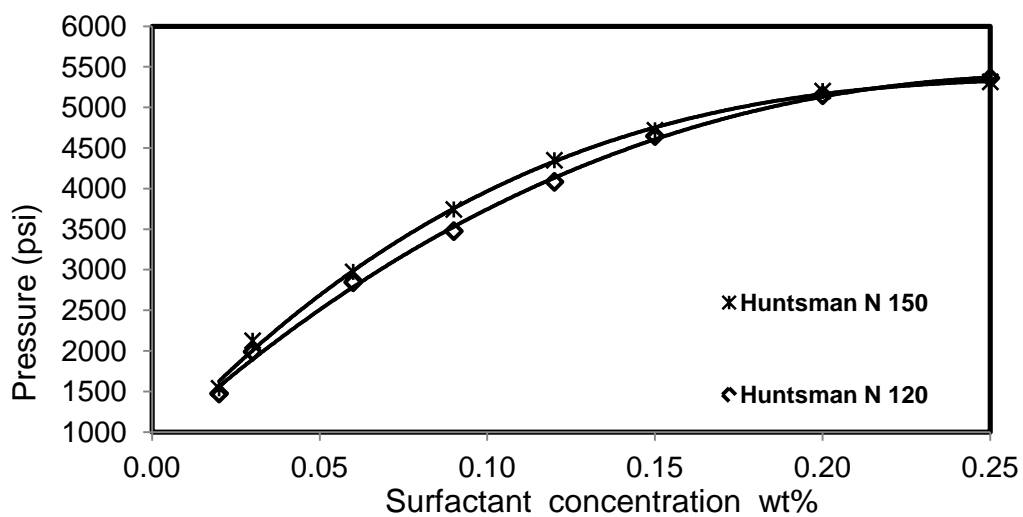


Figure 2. The solubility of SURFONIC® N-120 and N-150 in CO2 at 25 °C (Xing et al. 2010)

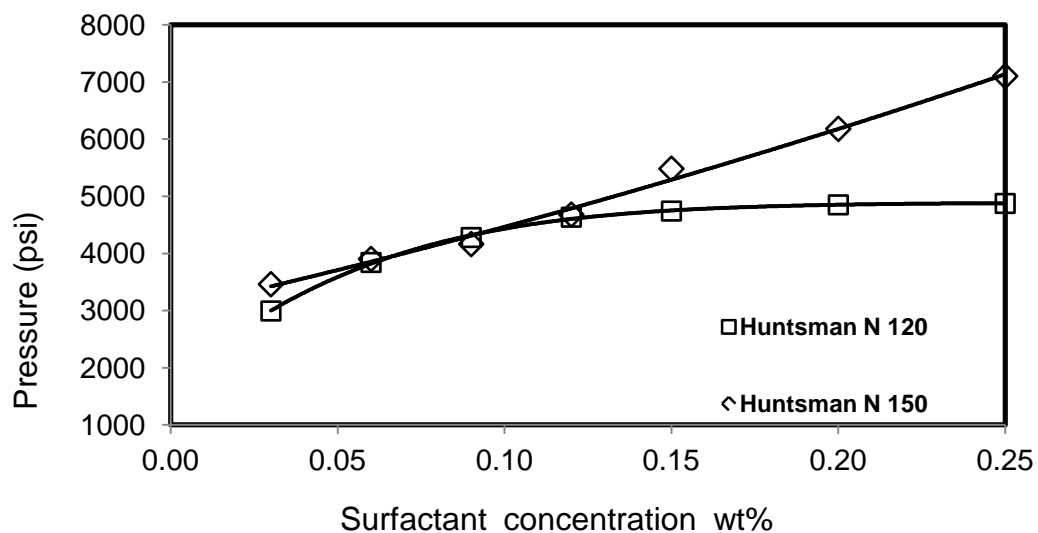


Figure 3. The solubility of SURFONIC® N-120 and N-150 in CO2 at 58 °C (Xing et al. 2010)

The branched nonylphenol ethoxylates yielded foams that were more stable than most of the other candidate surfactants, as shown in Figure 4. In-situ foam formation was also verified with transient mobility tests with a Berea sandstone core (104 mD) (Xing et al. 2011).

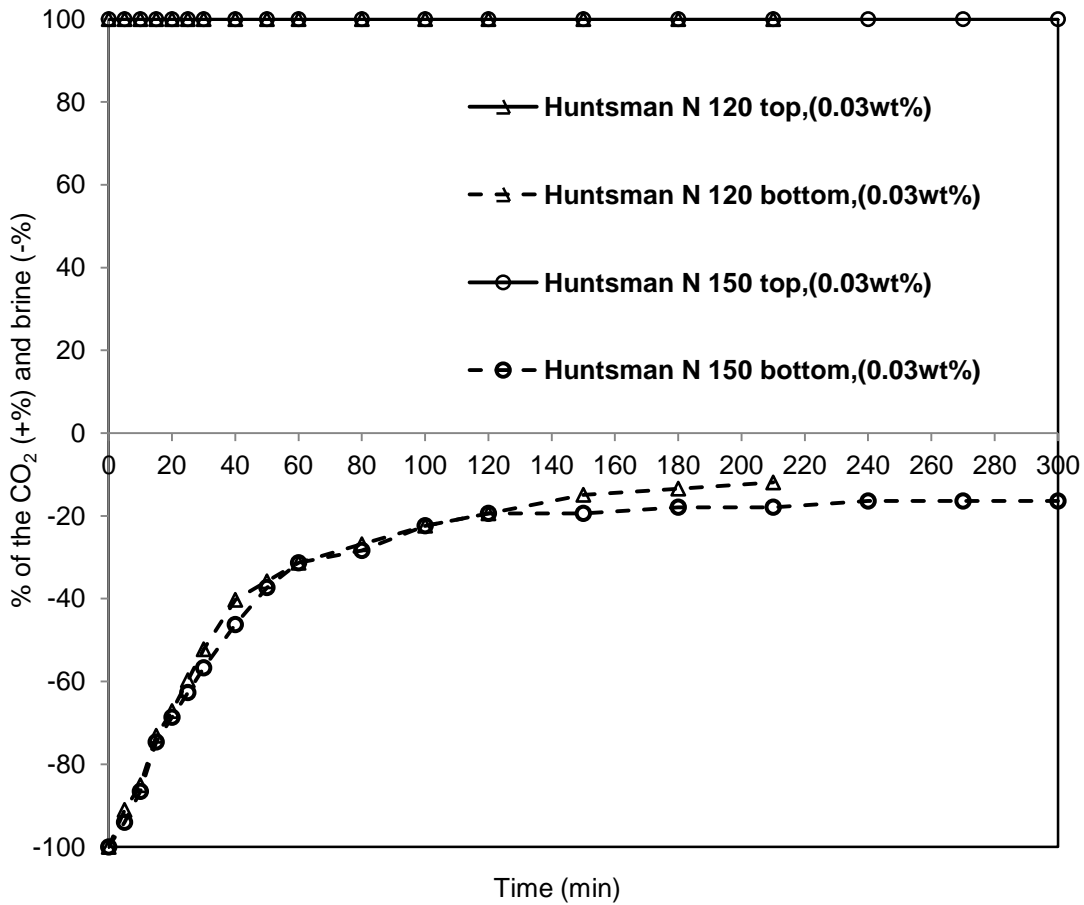


Figure 4. Foam stability associated with Huntsman SURFONIC® N-120 and N-150 surfactants at 1300 psia and 25 °C, with a brine (5wt%NaCl)/CO₂ volume ratio 1:1; 0.03% N-120 and N-150 based on CO₂ mass. At t=0 min, 100% of the CO₂ (top phase) and 100% of the brine (bottom phase) were in the foam. At t = ~120 min., 100% of the CO₂ and 20% of the brine were in the CO₂-in-brine foam, and 80% of the brine was in the excess brine phase. No excess CO₂ phase appeared up to 300 min. (Xing et al. 2010)

High pressure CO₂ was injected into the brine-saturated core and the corresponding pressure drop vs pore volumes injected (PVI) were recorded for experiments with no surfactant, surfactant only in the CO₂, surfactant only in the brine, and surfactant in both the brine and CO₂ Figure 5. The signature of in-situ foam generation is a significant increase in the pressure drop vs PVI results relative to the control displacement in which no surfactant is used (Farajzadeh et al. 2009). The pressure drop values when surfactant was dissolved in the CO₂ or the brine were at

least twice those attained when pure CO₂ was injected into the same brine-saturated core. The greatest increase in pressure was realized when the surfactant was present in both the CO₂ and brine.

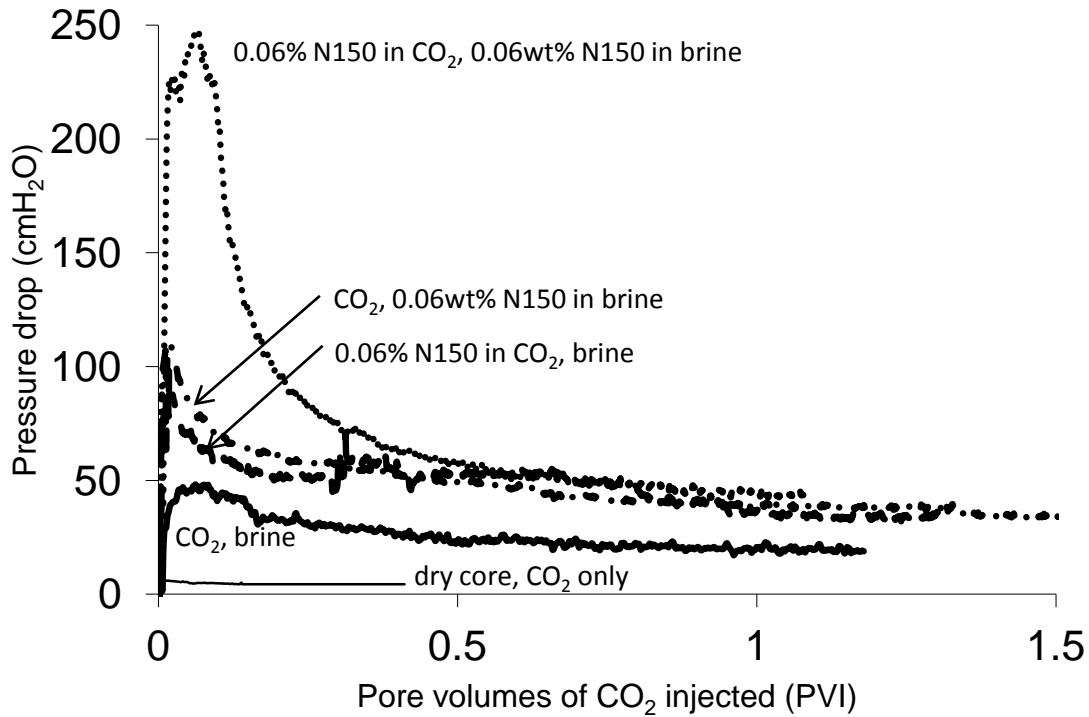


Figure 5. Pressure drop across a 6" long, 1" diameter, 104 md Berea sandstone core. 25 °C, ~2700 psi, 1 cm³/min volumetric flow rate (superficial velocity of 10 ft/day) (Xing et al. 2011)

CT imaging was also conducted with qa branched nonylphenol ethoxylate (Xing et al. 2011). In these tests, high pressure CO₂ invaded a polystyrene (PS) core (~30 mD) initially saturated with 5wt% KI brine because KI has a greater attenuation than NaCl (Wellington and Vinegar 1988), which created a greater contrast between brine and CO₂ in the scans. Further, the surfactant used in the CT imaging study was capable of stabilizing CO₂-in-5wt% TDS brine, whether the dissolved ion pair was NaCl or KI (Xing et al. 2011). The results indicated that despite the oil-wet nature of this medium, a sharp foam front propagated through the core and CO₂ fingers that formed in the absence of a surfactant (row A, Figure 6) were completely suppressed by foams formed due to the addition of 0.06wt% N-150 to the CO₂ (row C, Figure 6) or 1wt% N-150 to the brine (row B, Figure 6).

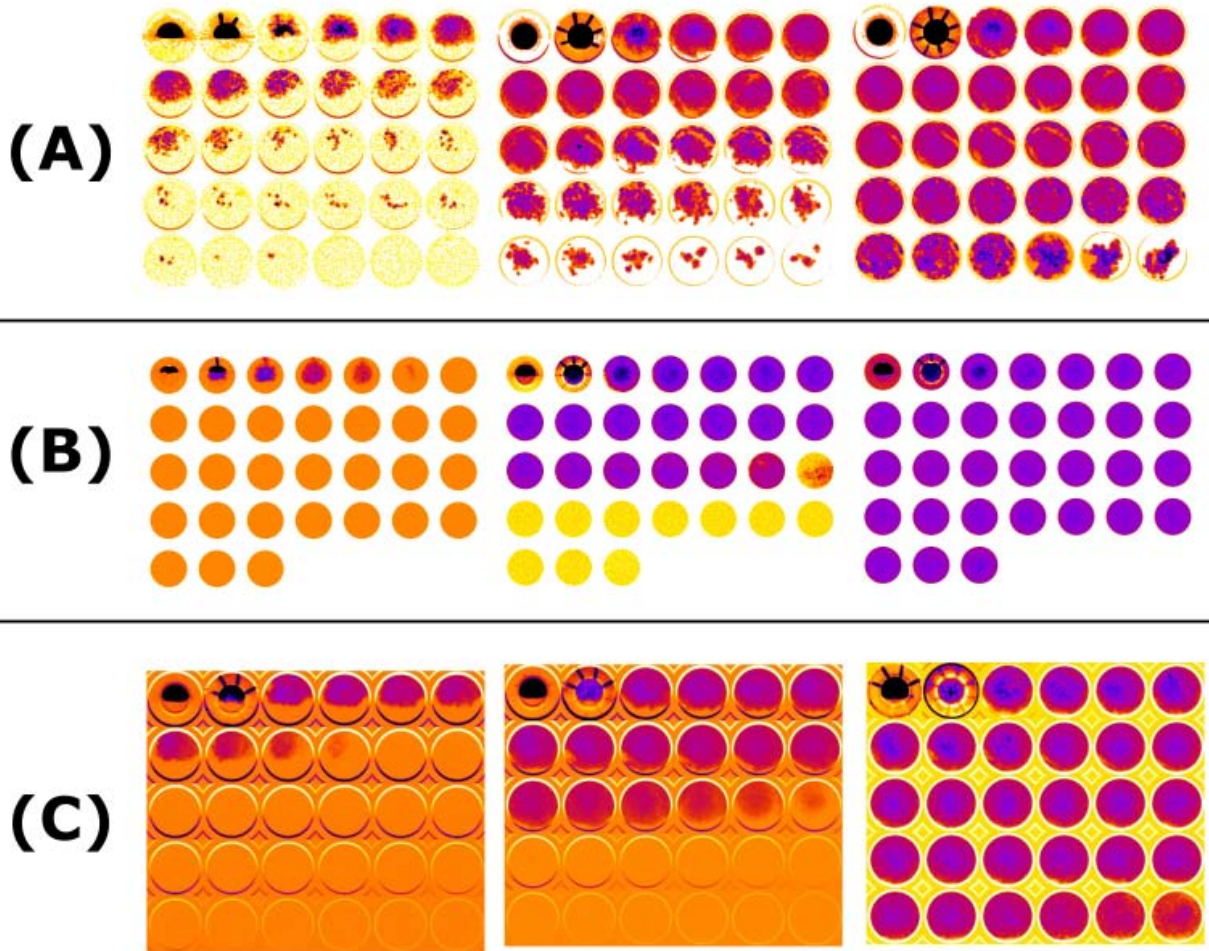


Figure 6a. CT slices of CO₂ within PS cores (~30 mD), ~2700 psi and 23°C; CO₂ inlet distributor at top left corner, move to the right for the next 5 slices, then to the next row, ending at the core outlet at bottom right corner. (A) no surfactant; (B) 1 wt% N-150 in brine; (C) 0.06 wt% N-150 in the CO₂. Superficial velocity of 0.83 ft/day.

Left column, scans for < 0.1 PVI. Middle column, scans for 0.1 < PVI < 0.2. Right column, scans for 0.2 < PVI and the saturation in the core was not observed to change dramatically afterward. False coloring applied to all images with darker colors indicating presence of CO₂

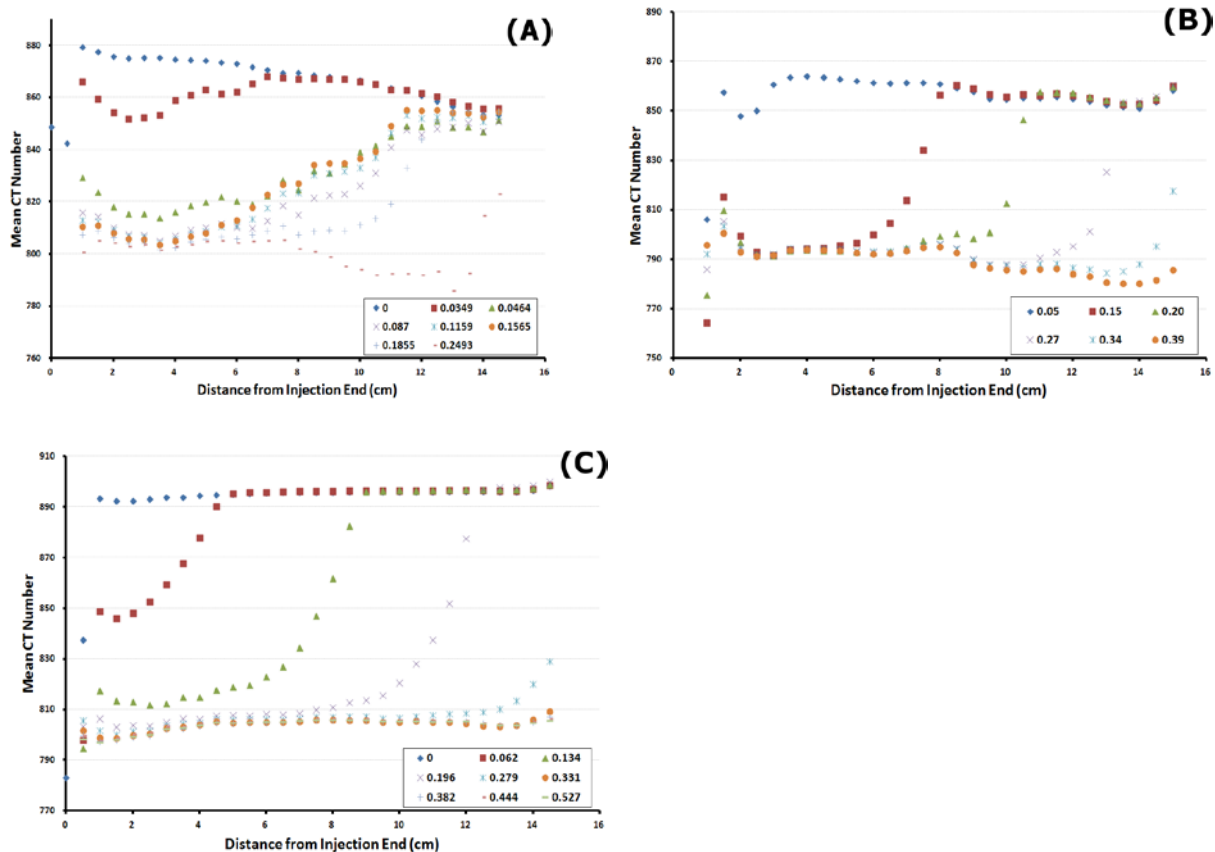


Figure 6b. Mean Coputed Tomography Number (CTN) along the length of the 6” PS core with CO₂ and brine with the legend indicating the number of PV injected at the beginning of each scan. Lower CTN indicates lower brine saturation and higher CO₂ saturation. (A) No surfactant (B) Surfactant dissolved in the brine (C) Surfactant dissolved in the injected CO₂.

In this study, additional transient mobility tests and CT imaging tests were conducted with the Huntsman SURFONIC® N-120 and N-150 surfactants. A synthetic SACROC brine (6.6wt% NaCl, 1.2wt% CaCl₂, 0.4wt% MgCl₂) was also used in some of the mobility tests.

3.0 EXPERIMENTAL

3.1 TRANSIENT MOBILITY (PRESSURE DROP) MEASUREMENTS; CO₂ INVADING BRINE-SATURATED BEREA SANDSTONE.

Flow-through-porous medium apparatus, rated to 4000 psi (27.7 MPa), was used to collect the pressure drop data for CO₂ flowing through a dry core, and for neat CO₂ or CO₂/surfactant solutions flowing into an initially brine-saturated or surfactant solution-saturated core at room temperature (~23°C). The core was wrapped in aluminum foil and then placed within a Buna-N sleeve. The core and sleeve were then placed inside the Temco [Model DCHR-1.0] core holder. Water was used as the overburden fluid to prevent annular flow of the fluids between the core and the inner surface of the sleeve. The overburden water pressure was maintained at ~500 psi (~3.5 MPa) above the CO₂ pressure by using a manual water pump [High Pressure Equipment Company Model 62-6-10]. CO₂ was initially pressurized to the desired pressure of ~2700 psia with a gas booster [Haskel Model AGD-75-C8], filling the windowed stirred cell [104 cm³, Thar Technologies Model R100], the core within the holder, the separator used to collect water that is displaced from the core, and the two coupled positive displacement pumps [Quizix, 270 cm³ per cylinder, Model C-6000-10K]. If surfactants were to be dissolved in the CO₂, the surfactants were loaded into the stirred cell prior to pressurization and mixed with CO₂ with the magnetically coupled stirrer until the solution was transparent.

During a mobility test, the first positive displacement pump was then engaged at a constant discharge volumetric flow rate, which resulted in the displacement of neat CO₂ from the pump into the continuously stirred cell. For tests conducted with surfactant initially dissolved in the CO₂ retained within the stirred cell, this resulted in a small amount of dilution of the surfactant solution. For example, the pore volume of a Berea core (104 mD) was only ~13 cm³ and the stirred cell volume was 104 cm³; therefore the injection of a pore volume of CO₂ into the stirred cell during the mobility test would reduce the surfactant concentration from 0.060wt% to 0.053wt%. The CO₂ or CO₂/surfactant solution leaving the stirred cell flowed into the core. The core effluent was directed into the separator [Swagelok, 300 cm³, Model 316L-50DF4-500] in which brine displaced from the core would accumulate. The CO₂ leaving the top of the separator was then received by the second positive displacement pump, which was

engaged at the same flow rate as the first pump but in the receiving mode. The CO₂ pressure was measured using the recycle pump analog transducers [Sensata Technologies] and the pressure transducers [Swagelok Model PTI-S-AG400-12AV] and the pressure drop along the core sample was measured by a differential pressure transducer [Validyne Model DP303-26]. The data acquisition was achieved using the Quizix and Validyne controllers and the National Instruments LabVIEW software. The cores used in the transient mobility tests include a water-wet Berea sandstone (104 mD), a water-wet Bentheimer sandstone (1550 mD), and two mixed wettability SACROC carbonate cores (8.9 mD and 3.6mD).

3.2 CT IMAGING OF CO₂ INVADING BRINE-SATURATED POLYSTYRENE CORES

A fourth-generation computed tomography (CT) scanner was used to image the CO₂-brine flow within initially brine-saturated polystyrene (PS) cores. Polystyrene cores were first used within the CT scanner were because of the lack of natural sub-core variations that are typically exhibited by sandstone or carbonate cores; the synthetic formation of the polystyrene cores creates a homogeneous porous media. The lack of channeling or preferential flow through bedding planes enables dynamic scanning of the front to be performed with greater ease within the CT scanner. The potential disadvantage of such a polymeric core is its oil-wet nature; in-situ foam-forming mechanisms are more conducive to water-wet porous media. Nonetheless foam generation has been previously reported using oil-wet models ([Lescure and Claridge 1986](#); [Romero and Kantzas 2004](#)) or dolomite cores ([Kuehne et al. 1992](#)).

Various PS cores with an internal pore structure similar in appearance to sandstone were used in this study (10s of mD, 10 - 20% porosity, 1" diameter). CT imaging was also performed on Berea sandstone cores (3-8 mD, 1.5" diameter). A 5 wt% potassium-iodide (KI) brine was used to initially saturate the cores prior to CO₂ injection. Injection of CO₂ injection was conducted at a constant flow rate such that the superficial velocity was in the 0.83 ft/day – 10 ft/day range. Pore pressure was about 2050 to 2200 psia (~14.1 – 15.2 MPa), with confining/overburden pressure maintained at a value about 250 psi (~1.7 MPa) above the pore pressure.

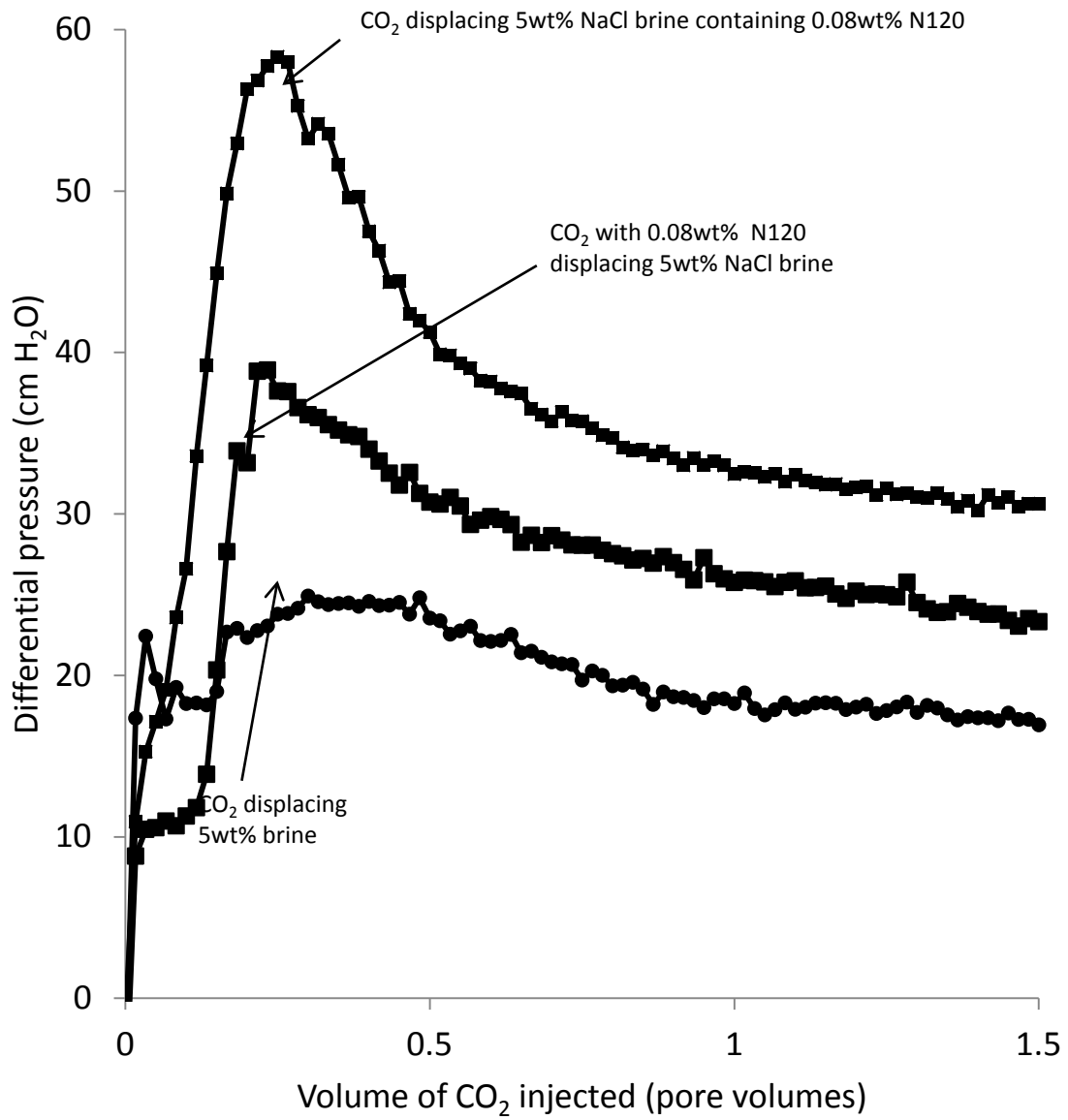
4.0 RESULTS

4.1 TRANSIENT MOBILITY MEASUREMENTS

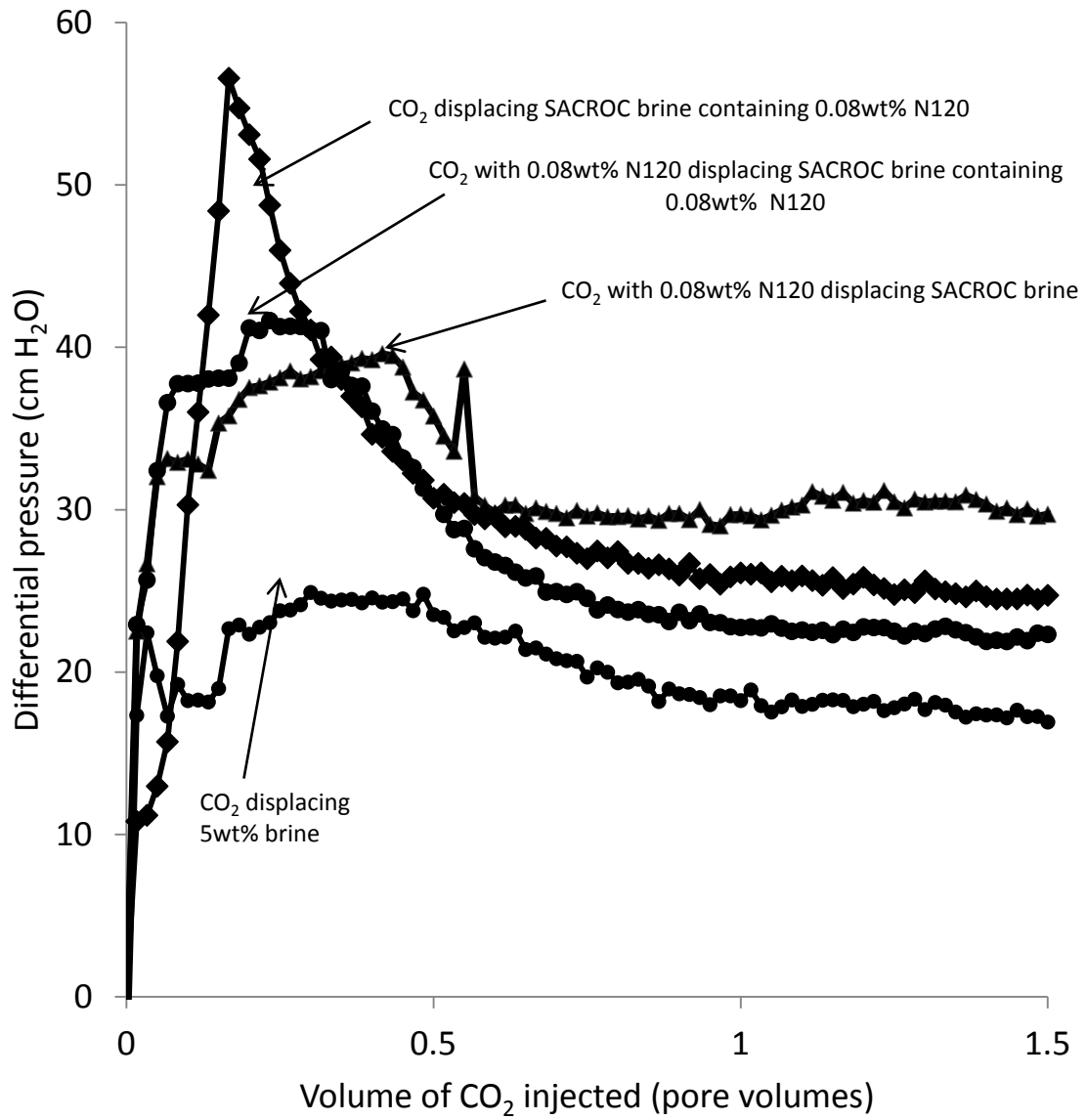
The pressure drop vs PVI profiles of the mobility tests conducted with a very high permeability (1500 mD) Bentheimer sandstone at a high superficial velocity (10 ft/day) indicate that foams were generated within the core whether the Huntsman SURFONIC N-120 surfactant was dissolved only in the CO₂, only in the brine, or in both the CO₂ and the brine, [Figure 7](#). The pressure drop across the core was roughly 2-3 times greater when surfactant was present relative to the control test that employed no surfactant in the CO₂ or the brine. This result, coupled with the similar results for a ~100 mD Berea sandstone shown in [Figure 6](#), indicate that CO₂-soluble surfactants seem to be capable of generating foams within relatively high permeability sandstone (>100 mD) at a high superficial velocity (10 ft/day).

Similar experiments were then conducted on a mixed wettability SACROC carbonate core (8.9 mD) at a superficial velocity of 10 ft/day. The results for the control test (no surfactant) and the experiments involving a 0.08wt% solution of Huntsman SURFONIC[®] N-120 or N-150 dissolved in the CO₂ are shown in [Figure 8](#). The increase in the pressure drop at equivalent PVI are more modest; a 20 – 50% increase in ΔP was observed when the surfactant was dissolved in the CO₂. When the surfactant was dissolved at 0.08wt% in the SACROC brine used to saturate the core, more substantial increases in pressure drop were observed, [Figure 9](#). The pressure drop values increased by a factor of 2-3 when the surfactant was dissolved in the brine.

When a lower permeability SACROC core was used (3.6 mD) in conjunction with the surfactant dissolved in the CO₂, modest increases in pressure drop (~15 – 50%) were observed at equivalent PVI relative to the results obtained using no surfactant, [Figure 10](#). (Tests with the surfactant dissolved in the brine that initially saturates this 3.6 mD core will be added to [Figure 10](#) in the conference presentation).



Figures 7a. Displacement of brine, either 5wt% NaCl or SACROC brine, with CO₂ at 21°C, 2700 psi. Bentheimer sandstone core (25% porosity, 1550 mD, 2.03" length, 1" diameter). CO₂ injection rate 1mL/min, 10 ft/day.



Figures 7b. Displacement of brine, either 5wt% NaCl or SACROC brine, with CO₂ at 21°C, 2700 psi. Bentheimer sandstone core (25% porosity, 1550 mD, 2.03" length, 1" diameter). CO₂ injection rate 1mL/min, 10 ft/day.

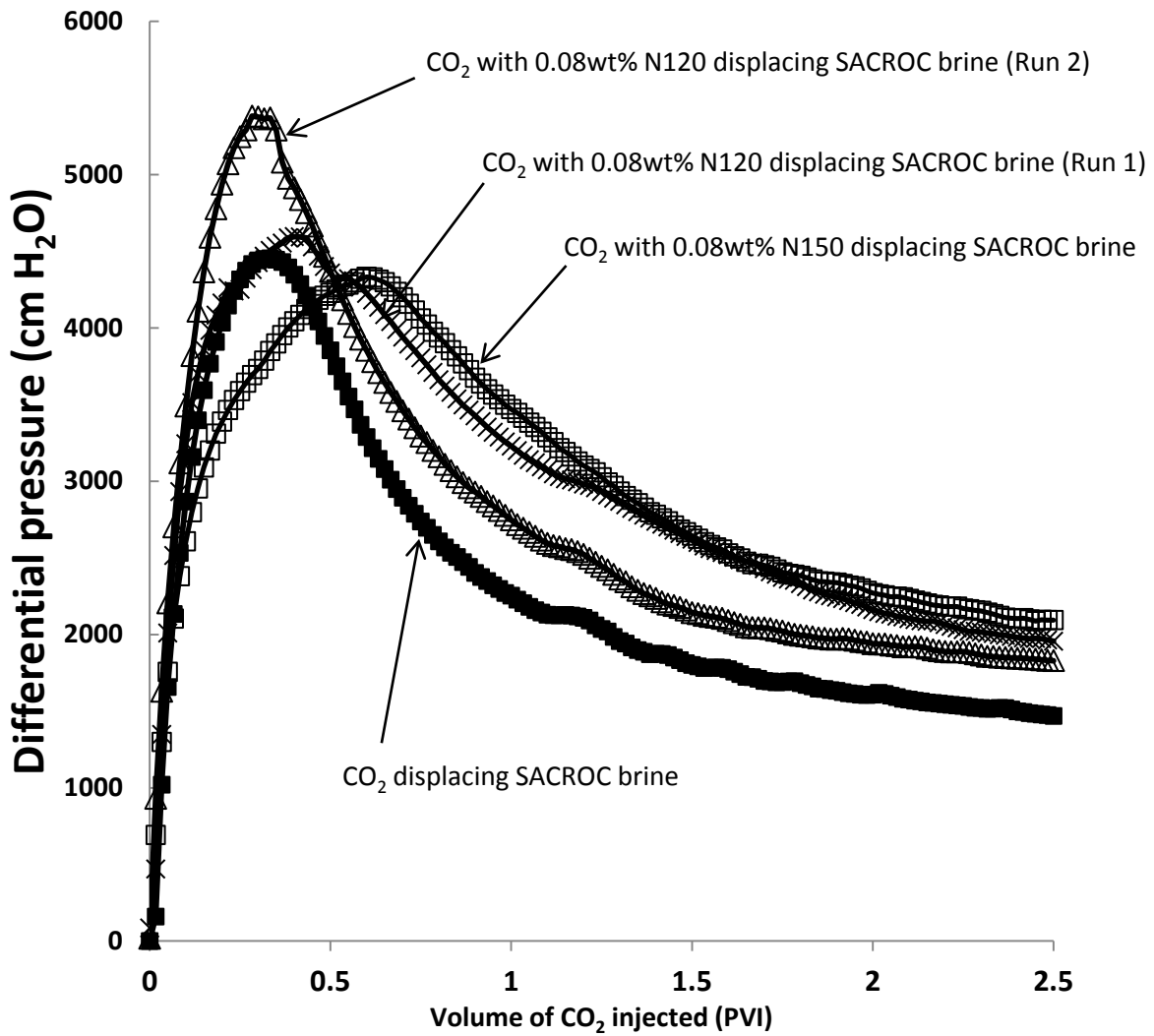


Figure 8. Displacement of SACROC brine (6.6wt% NaCl, 1.2wt% CaCl₂, 0.4wt% MgCl₂) with CO₂ at 21°C, 2700 psi. SACROC carbonate core (8.9mD, porosity 16.5%, 2.6" length, 1" diameter). Superficial velocity of 10 ft/day. Control test with no surfactant, and tests with surfactant in CO₂.

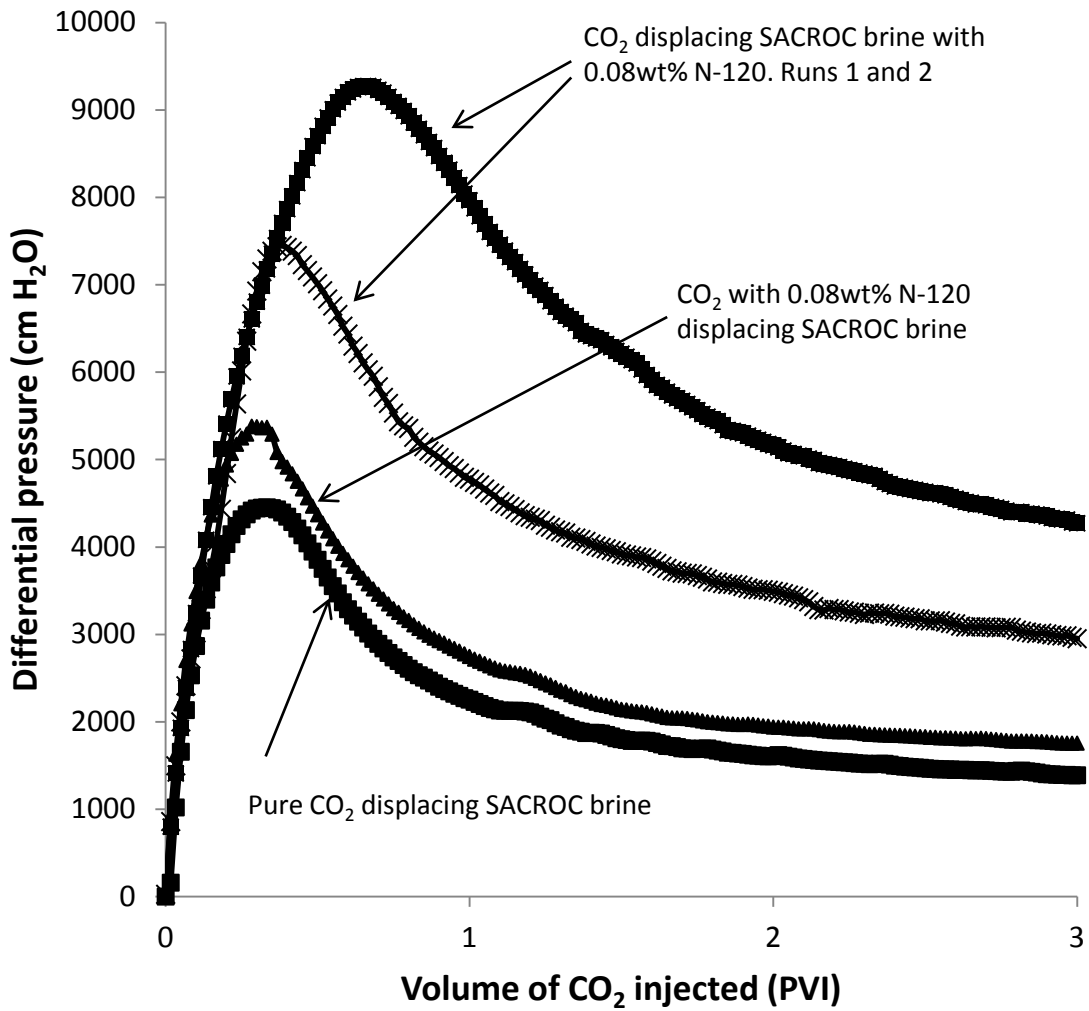


Figure 9. Displacement of SACROC brine (6.6wt% NaCl, 1.2wt% CaCl₂, 0.4wt% MgCl₂) with CO₂ at 21°C, 2700 psi. SACROC carbonate core (8.9mD, porosity 16.5%, 2.6" length, 1" diameter). Superficial velocity of 10ft/day. Control test with no surfactant, a test with surfactant in CO₂, and tests with surfactant in brine.

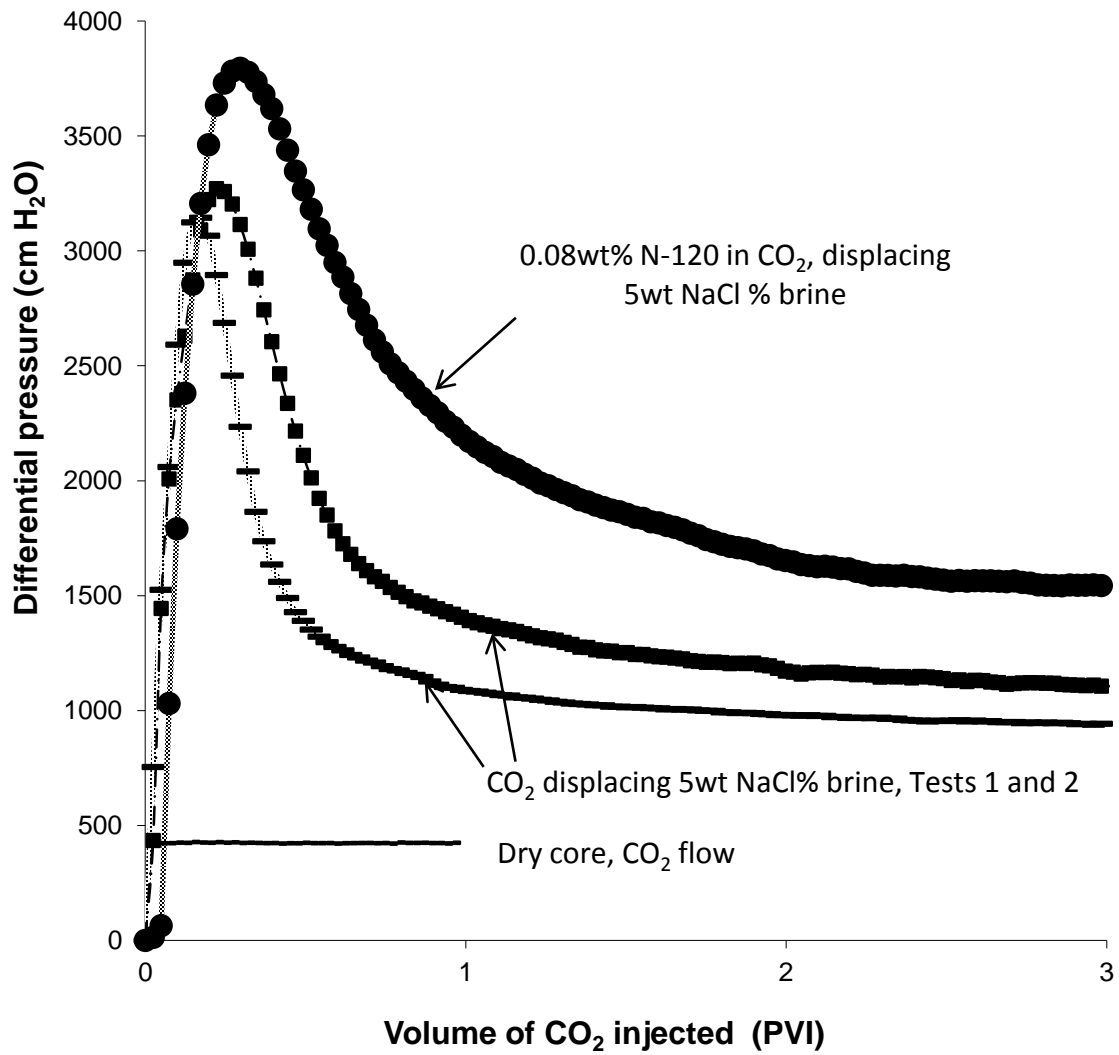


Figure 10. Displacement of 5wt% NaCl brine with CO₂ at 21°C, 2700 psi. SACROC carbonate core (3.6mD, porosity 14% porosity, 2" length, 1" diameter). Superficial velocity of 10 ft/day. Control tests with no surfactant, and a test with surfactant in CO₂.

4.2 CT IMAGING

The first set of CT tests (designated SS 103, 104 and 108) were relatively low flow rate tests (0.47 ft/day) conducted with in Berea sandstone (3 - 5 mD) to assess the effects of no surfactant (SS 103, Figure 11), SURFONIC[®] N-150 dissolved only in the brine that initially saturated the core (SS 103, Figure 12), and SURFONIC[®] N-150 dissolved only in the CO₂ that is injected into the core (SS 108, Figure 13). The cross-sectional images of control test results with no surfactant (SS 103, Figure 11) illustrate the preferential flow of CO₂ through high permeability planes within the core. The plot of mean CT number vs slice number/position down the length of the core shows a gradual increase from a low CTN number (CO₂-rich) to higher average CT number (brine-rich). No sharp transition is evident from a CO₂-rich region to a brine-rich region that would be characteristic of foam, and none was expected. When the surfactant was dissolved in the brine (SS 104, Figure 12), however, the cross-sectional plots illustrate a more uniform distribution of CO₂ in the cross-section, especially near the core inlet. The mean CT number vs length data display a relatively sharp increase from low values to high values. Both of these results indicate that foam was generated at a relatively low flow rate when the surfactant was dissolved in the brine, and the foam was capable or propagating through the core. When the surfactant was dissolved only in the CO₂ (SS 108, Figure 13), however, the results were comparable to the trends observed in the control experiment (SS 103, Figure 11), indicating that little if any foam was generated in the Berea sandstone at a lower superficial velocity.

The second set of CT tests (designated SS 106, 113, 107, 112, 109) correspond to relatively high flow rate tests (superficial velocity of 4.7 ft/day) in Berea sandstone (4 – 8 mD) with no surfactant (control, SS 106, Figure 14), SURFONIC[®] N-120 in the brine (SS 113, Figure 15), SURFONIC[®] N-150 in the brine (SS 107, Figure 16), SURFONIC[®] N-120 in the CO₂ (SS 112, Figure 17), and SURFONIC[®] N-150 in the CO₂ (SS 109, Figure 18). As expected, the displacement with no surfactant present is characterized by the lack of a foam front and by the flow of CO₂ through the higher permeability bedding planes (Figure 14). Upon the addition of surfactant to the brine, foams are generated in-situ, Figures 15 and 16. The foam formed with SURFONIC[®] N-150 present in the brine, Figure 16, is particularly distinct as evidenced by a nearly step-like change in average CT number from low values that correspond to the CO₂-rich foam to high values that correspond to the brine, and by cross-sectional slices that

appear to be completely swept by the CO₂ behind the front. When the surfactant was present only in the injected CO₂, foam-like fronts were also generated, especially near the core inlet, [Figures 17 and 18](#). The foam-front was not as distinct as that observed when the SURFONIC[®] N-150 present only in the brine, [Figure 16](#). (No CT imaging tests have yet been conducted with surfactant in both the brine and the CO₂). CT tests in Berea SS are summarized in [Table 1](#).

Table 1. Conditions for CT imaging displacements, 23 °C 2200 or 2300 psi, CO₂ invading a 5wt% KI brine-saturated Berea sandstone core; *permeability values for all cores not measured, those cores were estimated to be ~20% porous and ~5 mD

CT test	Surfact	Phase surfact. dissolved in	Surfact Conc Wt%	Injection rate ml/min	Superficial velocity ft/day	Core Diam inches	Core length inches	Core perm mD	Core porosity %	Core PV ml
SS 103	none	-	-	0.2	0.47	1.99	6.05	4.7	19.9	61.27
SS 104	N-150	brine	0.10	0.2	0.47	1.99	6.21	3.2	19.4	61.39
SS 108	N-150	CO ₂	0.06	0.2	0.47	1.99	6.13	3.0	19.8	61.41
SS 106	none	-	-	2.0	4.7	1.97	6.12	6.0	18.0	55.32
SS 113	N-120	brine	0.10	2.0	4.7	2.01	5.16	5*	20*	53.10
SS 107	N-150	brine	0.02	2.0	4.7	1.99	6.10	3.9	19.6	60.82
SS 112	N-120	CO ₂	0.06	2.0	4.7	1.99	6.13	7.6	19.8	60.88
SS 109	N-120	CO ₂	0.06	2.0	4.7	1.99	6.08	6.1	19.5	60.32

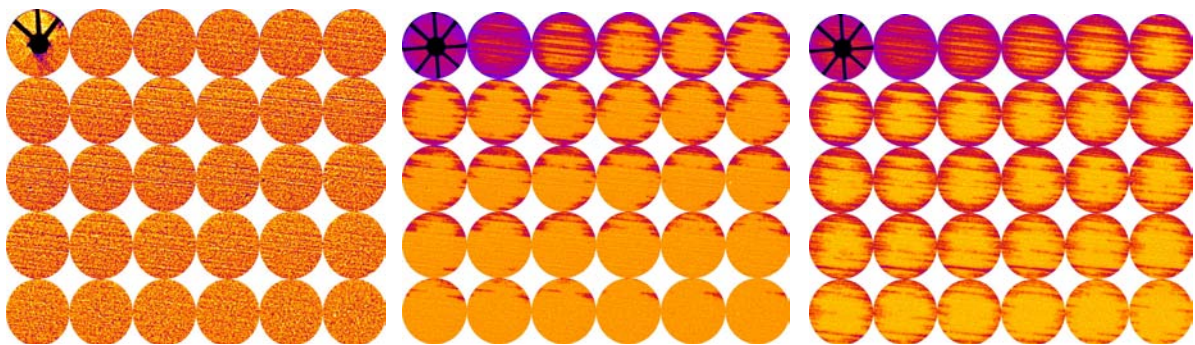
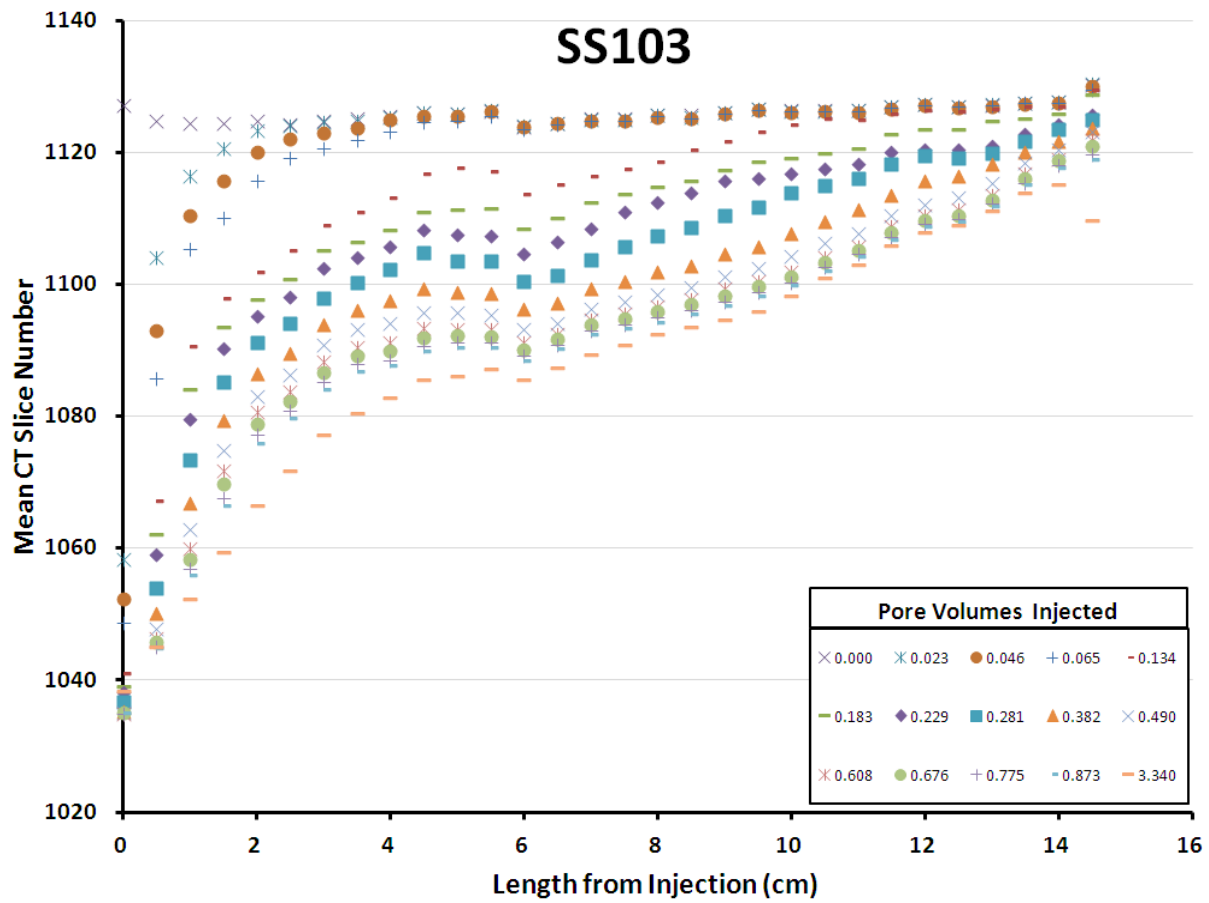


Figure 11. Low flow rate test (0.2 ml/min, 0.47 ft/day) in low permeability Berea sandstone (4.7 mD); control test with no surfactant and no foam; Above: plots of mean CT number for the cross-section vs position at various PVI; low values are CO₂-rich, high values are brine-rich. Below: Montages of cross-sectional slices (left to right) correspond to 0 PVI (wet), 0.183 PVI, and 3.34 PVI; purple is CO₂-rich. Inlet distributor at top left corner, move to the right for the next 5 slices, then to the next row, ending at the core outlet at bottom right corner.

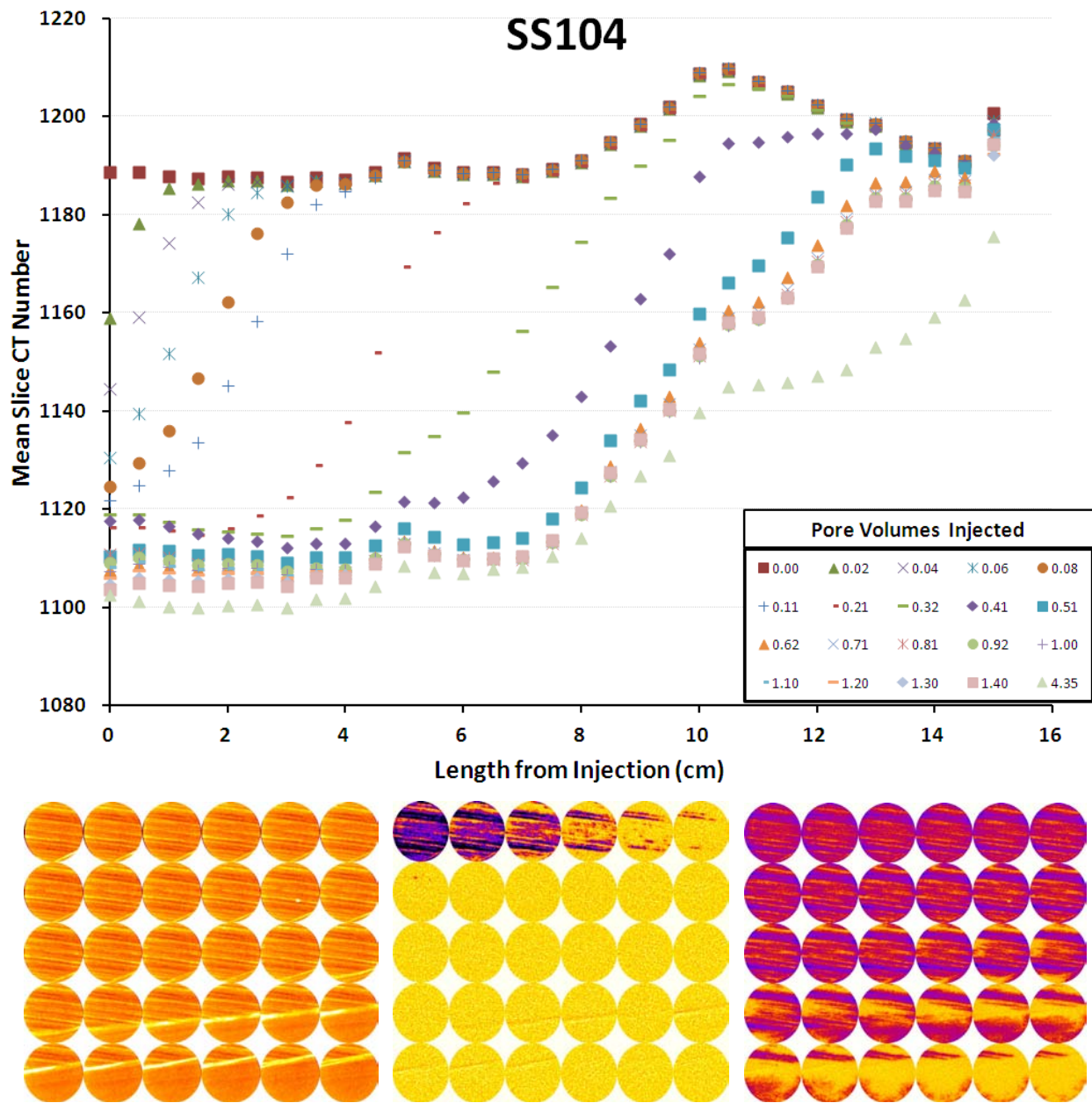


Figure 12. Low flow rate test (0.2 ml/min, 0.47 ft/day) in low permeability Berea sandstone (3.2 mD); surfactant N-150 in brine; Above: plots of mean CT number for the cross-section vs position at at various PVI; low values are CO₂-rich, high values are brine-rich. Below: Montages of cross-sectional slices (left to right) correspond to 0 PVI (wet), 0.060 PVI, and 1.30 PVI; purple is CO₂-rich. Inlet distributor at top left corner, move to the right for the next 5 slices, then to the next row, ending at the core outlet at bottom right corner.

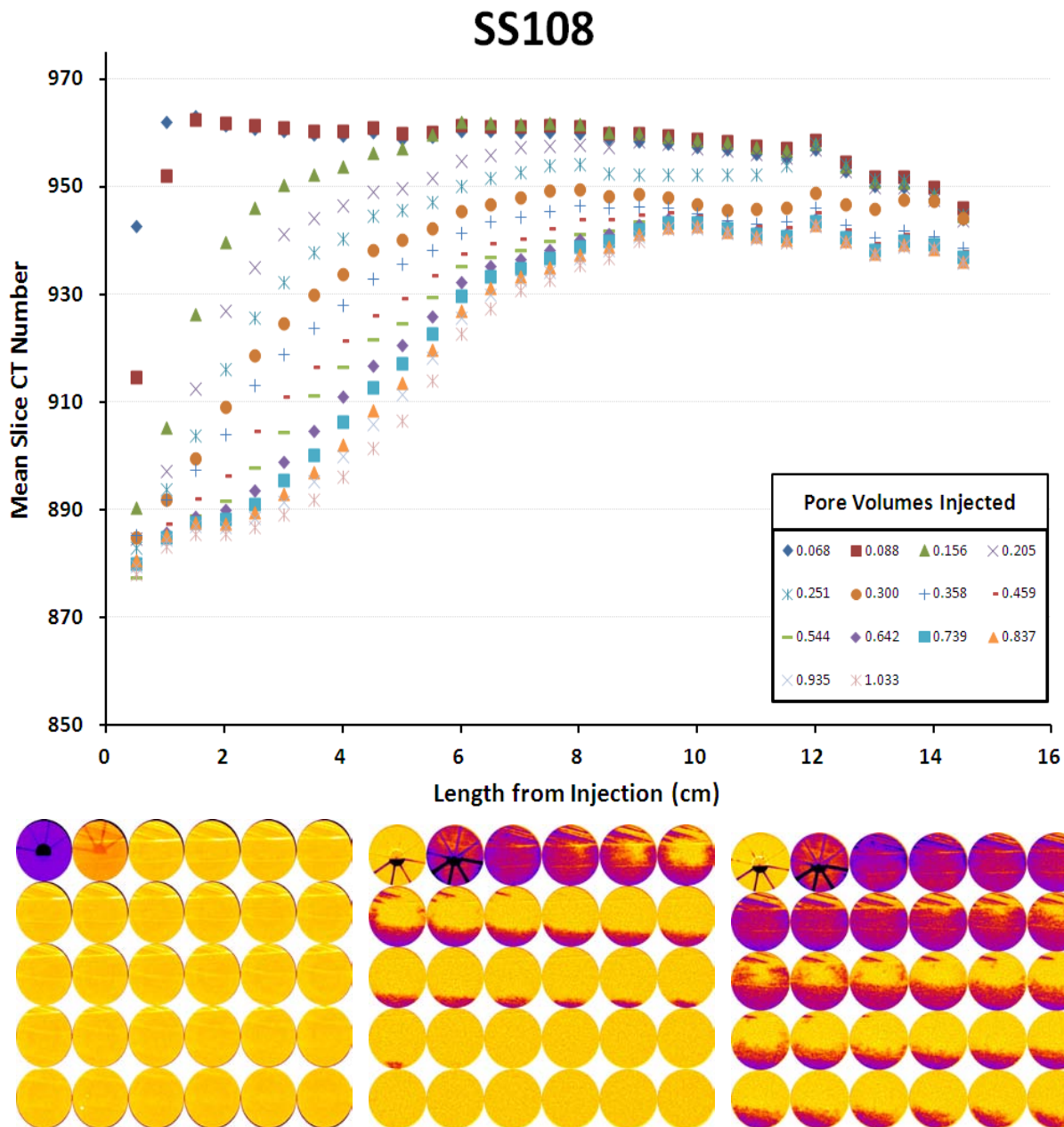


Figure 13. Low flow rate test (0.2 ml/min, 0.47 ft/day) in low permeability Berea sandstone (3.0 mD); surfactant N-150 in CO₂;
 Above: plots of mean CT number for the cross-section vs position at various PVI; low values are CO₂-rich, high values are brine-rich. Below: Montages of cross-sectional slices (left to right) correspond to 0 PVI (wet), 0.060 PVI, and 1.30 PVI; purple is CO₂-rich. Inlet distributor at top left corner, move to the right for the next 5 slices, then to the next row, ending at the core outlet at bottom right corner.

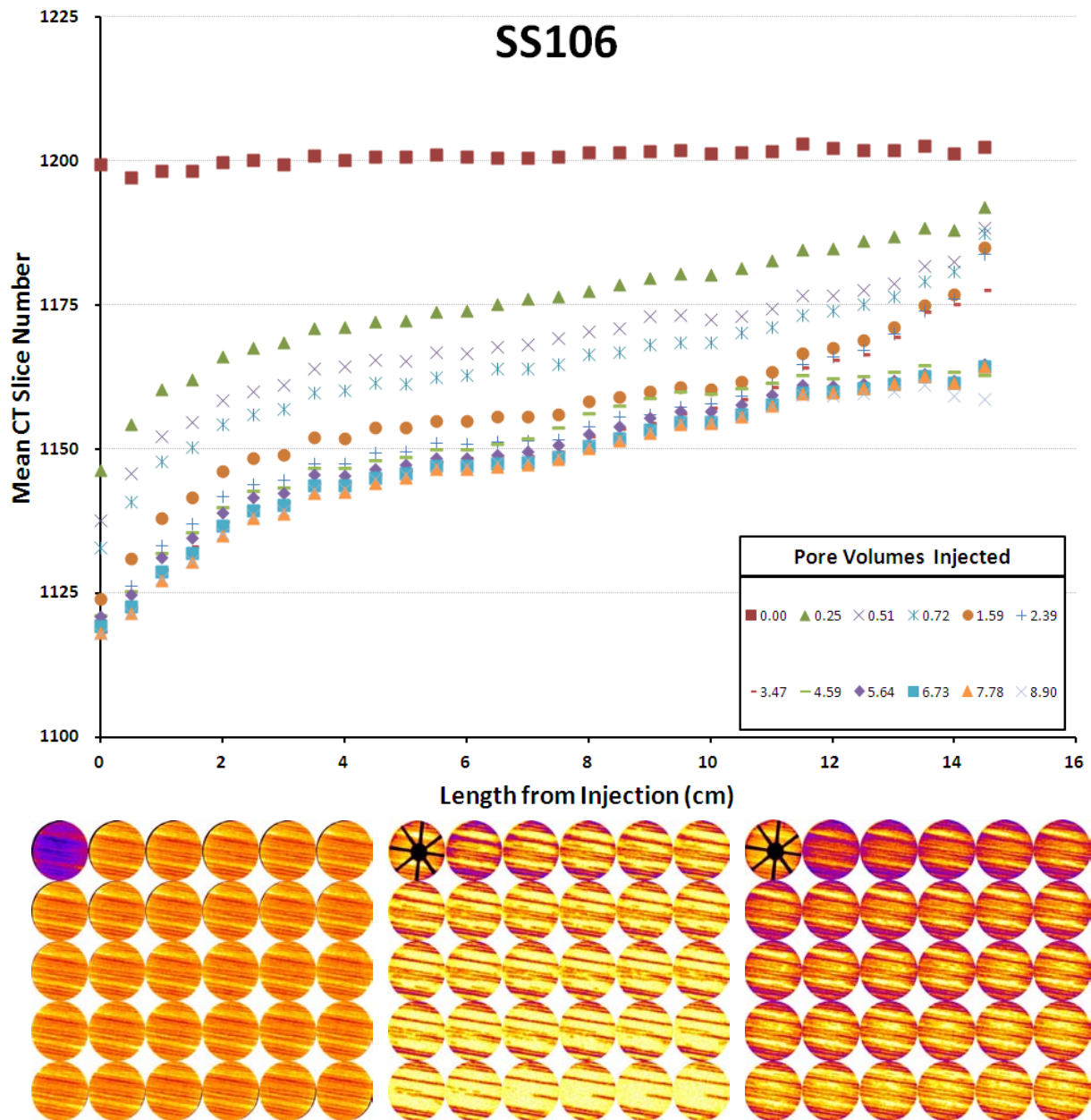


Figure 14. High flow rate test (2.0 ml/min, 4.7 ft/day) in low permeability Berea sandstone (6.0 mD); control test with no surfactant and no foam; Above: plots of mean CT number for the cross-section vs position at various PVI; low values are CO₂-rich, high values are brine-rich. Below: Montages of cross-sectional slices (left to right) correspond to 0 PVI (wet), 0.25 PVI, and 8.9 PVI; purple is CO₂-rich. Inlet distributor at top left corner, move to the right for the next 5 slices, then to the next row, ending at the core outlet at bottom right corner.

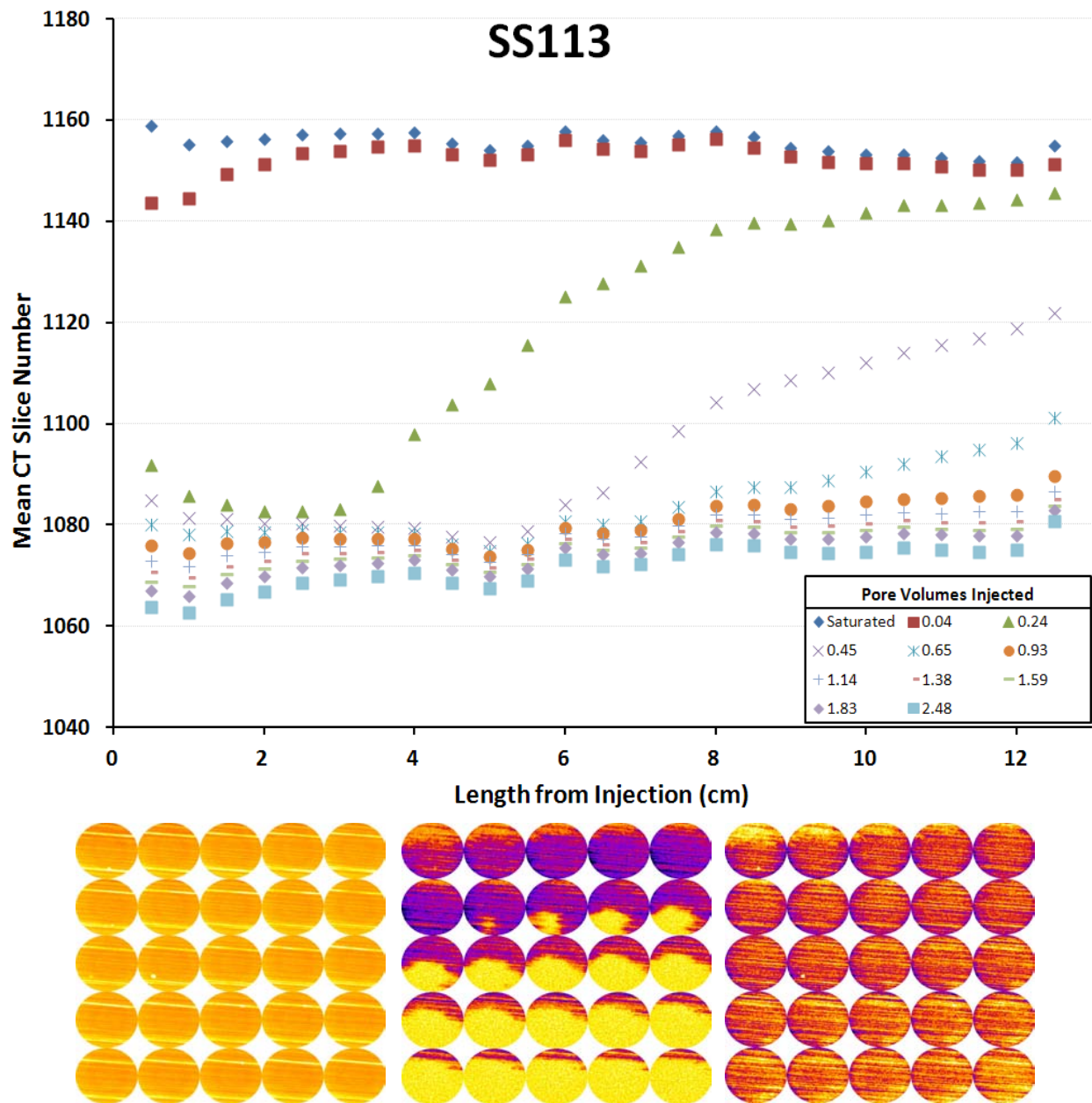


Figure 15. High flow rate test (2.0 ml/min, 4.7 ft/day) in low permeability Berea sandstone (~5 mD); surfactant N-120 in brine; Above: plots of mean CT number for the cross-section vs position at various PVI; low values are CO₂-rich, high values are brine-rich. Below: Montages of cross-sectional slices (left to right) correspond to 0 PVI (wet), 0.24 PVI, and 1.30 PVI; purple is CO₂-rich. Inlet distributor at top left corner, move to the right for the next 5 slices, then to the next row, ending at the core outlet at bottom right corner.

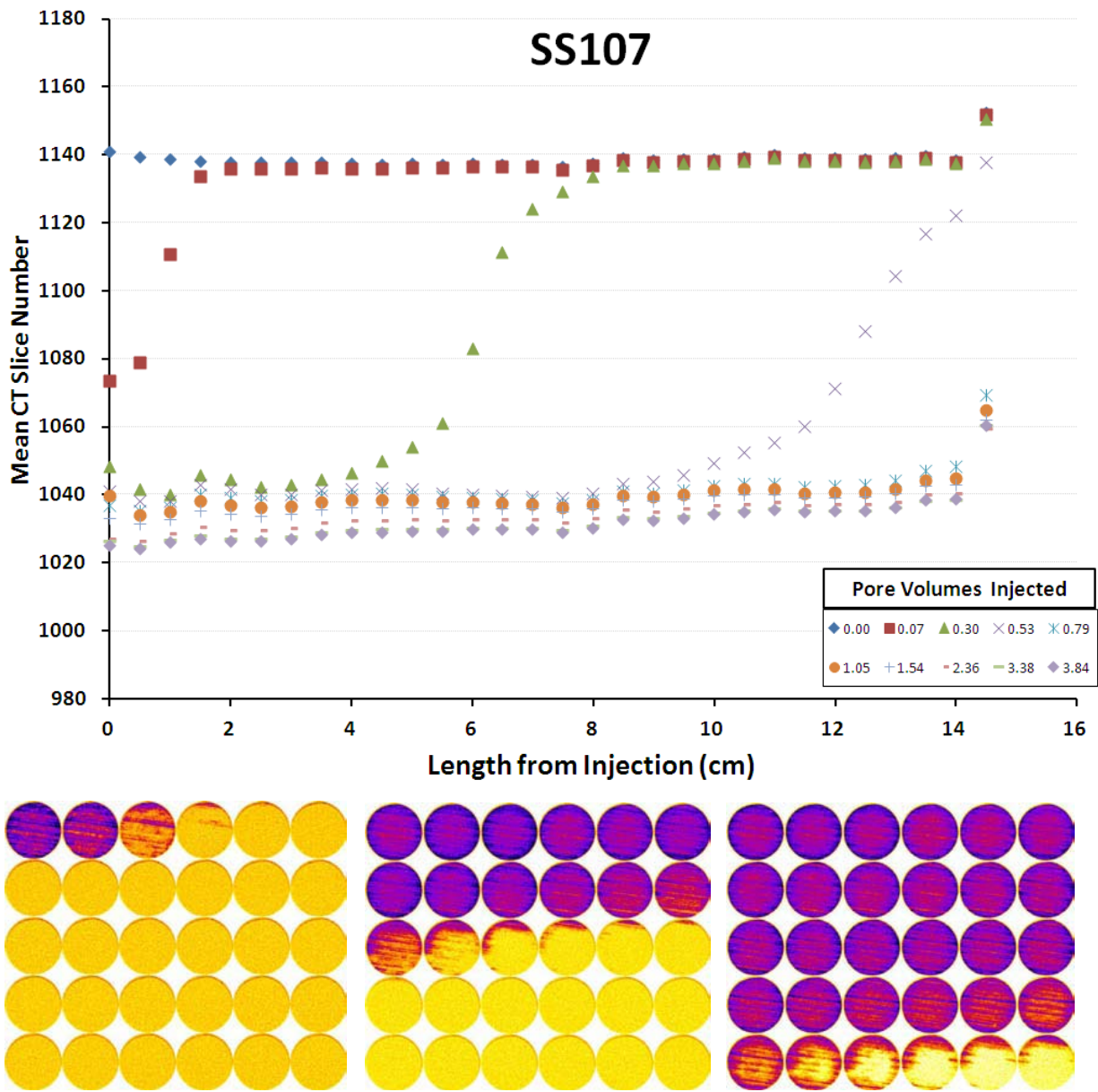


Figure 16. High flow rate test (2.0 ml/min, 4.7 ft/day) in low permeability Berea sandstone (3.9 mD); surfactant N-150 in brine; Above: plots of mean CT number for the cross-section vs position at various PVI; low values are CO₂-rich, high values are brine-rich. Below: Montages of cross-sectional slices (left to right) correspond to 0.07 PVI, 0.30 PVI, and 0.53 PVI; purple is CO₂-rich. Inlet distributor at top left corner, move to the right for the next 5 slices, then to the next row, ending at the core outlet at bottom right corner.

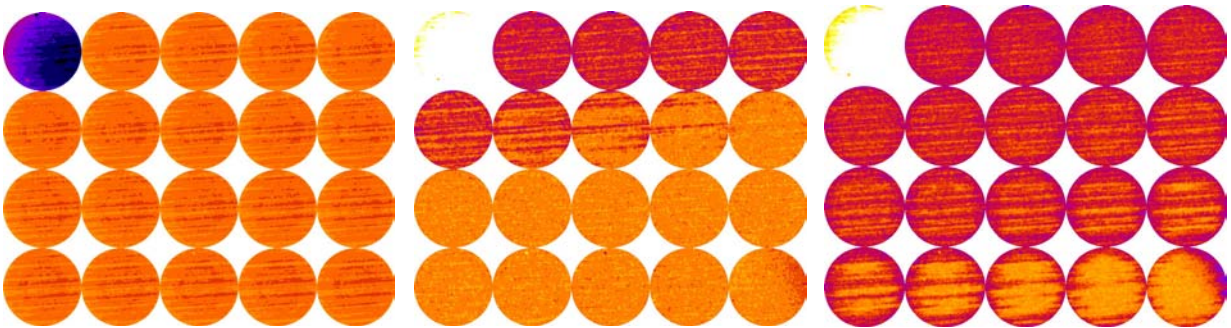
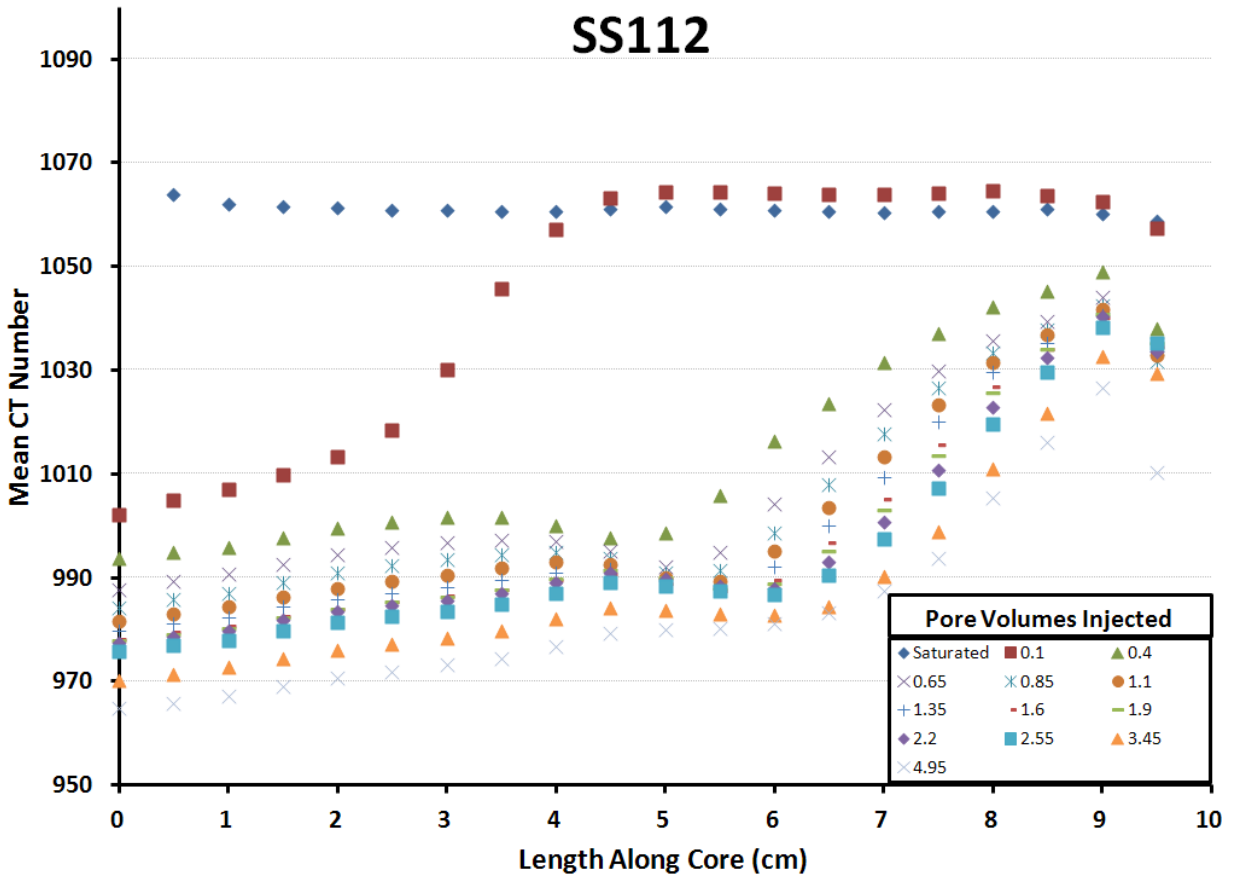


Figure 17. High flow rate test (2.0 ml/min, 4.7 ft/day) in low permeability Berea sandstone (7.6 mD); surfactant N-120 in CO₂;
 Above: plots of mean CT number for the cross-section vs position at at various PVI; low values are CO₂-rich, high values are brine-rich. Below: Montages of cross-sectional slices (left to right) correspond to 0 PVI (wet), 0.10 PVI, and 3.45 PVI; purple is CO₂-rich. Inlet distributor at top left corner, move to the right for the next 5 slices, then to the next row, ending at the core outlet at bottom right corner.

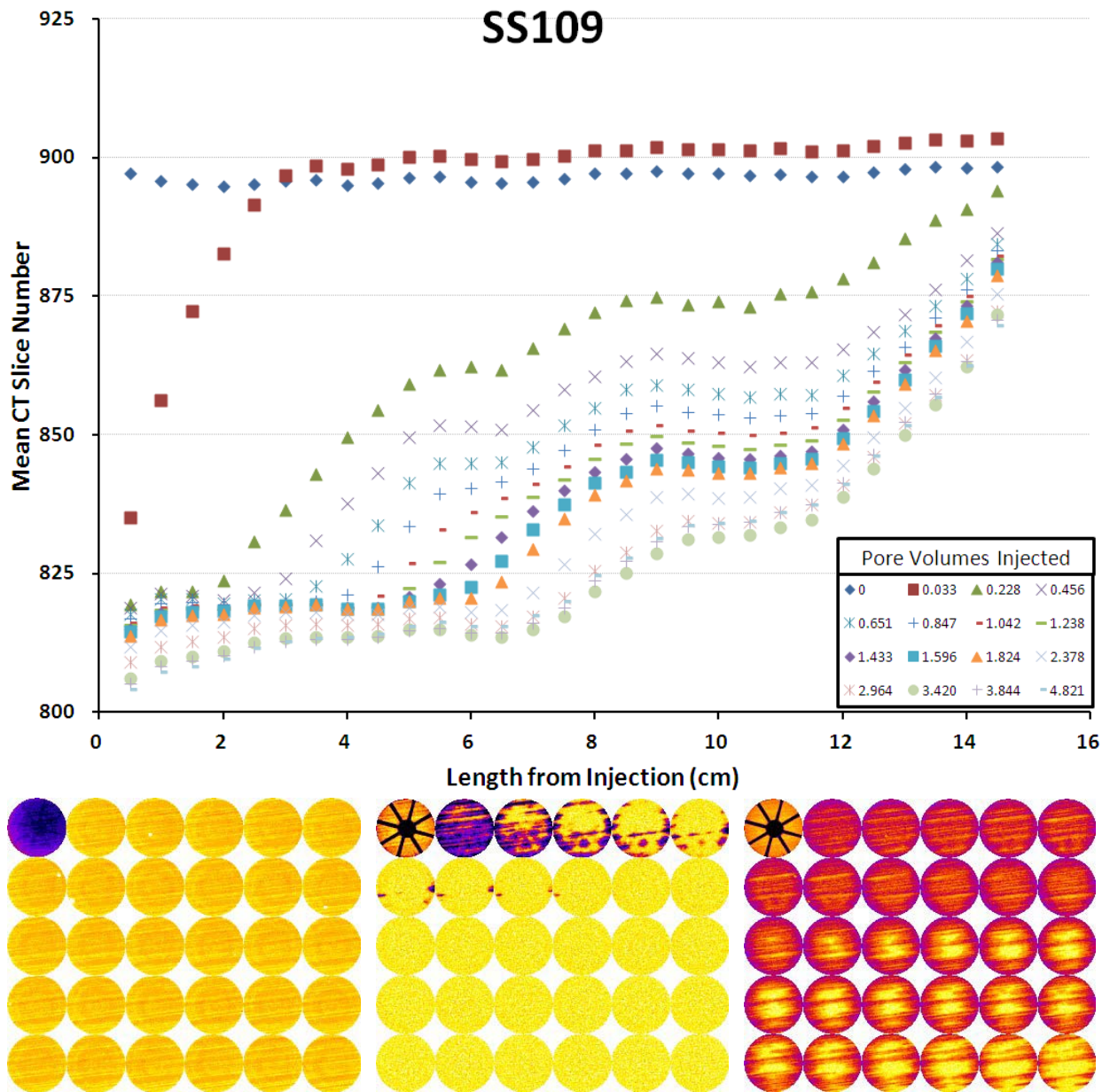


Figure 18. High flow rate test (2.0 ml/min, 4.7 ft/day) in low permeability Berea sandstone (6.1 mD); surfactant N-120 in CO₂; Above: plots of mean CT number for the cross-section vs position at various PVI; low values are CO₂-rich, high values are brine-rich. Below: Montages of cross-sectional slices (left to right) correspond to 0 PVI (wet), 0.033 PVI, and 1.596 PVI; purple is CO₂-rich. Inlet distributor at top left corner, move to the right for the next 5 slices, then to the next row, ending at the core outlet at bottom right corner.

5.0 CONCLUSIONS

Commercially available, water-soluble, slightly CO₂-soluble nonionic surfactants capable of dissolving sufficiently in dense CO₂ to generate and stabilize CO₂-in-brine foams have recently been identified. Our prior studies (Xing et al. 2010; Xing et al. 2011) detailed the solubility of numerous non-ionics in CO₂ and assessed their ability to stabilize foams in a high pressure windowed vessel. The transient mobility tests and CT imaging analysis results of this study have indicated that foams can also be generated in porous media when the CO₂-surfactant solution flows into a core initially saturated with brine. Two highly branched nonylphenol ethoxylates with an average of 12 or 15 ethylene oxide groups in the hydrophilic tail, Huntsman SURFONIC[®] N-120 and N-150, were selected for the study.

The mobility results for the water-wet, relatively high permeability sandstones (104 mD Berea, and 1550 mD Bentheimer) at a superficial velocity of 10 ft/day indicated that foams were readily generated in-situ when the surfactant was dissolved in the CO₂, the brine, or both the CO₂ and the brine. The pressure drop across the core increased by roughly a factor of 2-3 during the injection of the first few pore volumes of CO₂, and the magnitude of the mobility decrease was comparable whether the surfactant was present in the CO₂ or the brine. When mixed wettability SACROC carbonate cores (3.6 and 8.9 mD) were used, however, the mobility decrease was more modest relative to the control test with no surfactant when the surfactant was dissolved in the CO₂, as evidenced by 20 – 50 % increases in pressure drop. Stronger foams (2 – 3-fold increases in pressure drop) were generated when the surfactant was present in the brine phase in the only SACROC core tested under these conditions (8.9 mD).

CT imaging indicated the in-situ foam formation and propagation occurred at low flow rates (0.47 ft/day) in Berea sandstone (4 – 8 mD) most readily if the surfactant is present in the brine. Foam formation was not apparent when the surfactant was dissolved in the CO₂. At higher flow rates (4.7 ft/day), however, foam formation and propagation was observed whether the surfactant was dissolved in the CO₂ or the brine.

These results indicate that commercially available, non-ionic, slightly CO₂-soluble, water-soluble surfactants appear to be promising chemicals for improving mobility control during CO₂ floods. CO₂-soluble surfactants provide operators with the opportunity to inject the surfactant dissolved in the injected CO₂, or (because they are

also water-soluble) dissolved in both in brine slugs and CO₂ slugs, rather than relying solely on the alternating injection of aqueous surfactant solutions and CO₂ (SAG) to form conformance and/or mobility control foams.

BIBLIOGRAPHY

- Adkins, S.S.; Chen, X.; Chan, I.; Torino, E.; Nguyen, Q.; Sanders, A.; Johnston, K.; Morphology and Stability of CO₂-in-Water Foams with Nonionic Hydrocarbon Surfactants; *Langmuir* 2010; 26(8) 5335–5348
- Bernard, G.; Holm, L.; Method for recovering oil from subterranean formations; U.S. Patent 3,342,256; issued Sept. 19, 1967
- daRocha, S.; Psathus, P.; Klein, E.; Johnston, K.; Concentrated CO₂ in Water Emulsions with Nonionic Polymeric Surfactants; *Journal of Colloid and Interface Science* 2001; (239) 241-253
- Dhanuka, V.; Dickson, J.; Ryoo, W.; Johnston, K.; High internal phase CO₂-in-water emulsions stabilized with a branched nonionic hydrocarbon surfactant; *Journal of Colloid and Interface Science* 2006; (298) 406-418
- Enick, R.; Olsen, D.; Mobility and Conformance Control for Carbon Dioxide Enhanced Oil Recovery (CO₂-EOR) via Thickeners, Foams, and Gels – A Detailed Literature Review of 40 Years of Research; DOE/NETL-2012/1540, Activity 4003.200.01, 2011
- Fan, X.; Potluri, V.; McLeod, M.; Wang, Y.; Liu, J.; Enick, R. M.; Hamilton, A.; Roberts, C.; Johnson, J.; Beckman, E.; Oxygenated Hydrocarbon Ionic Surfactants Exhibit CO₂ Solubility; *J. Am. Chem. Soc.* 2005; 127(33)11754-11762
- Farajzadeh, R.; Andrianov, A.; Zitha, P.L.J.; Foam Assisted Enhanced Oil Recovery at Miscible and Immiscible Conditions; presented at the 2009 SPE Kuwait International Petroleum Conference and Exhibition; held in Kuwait City, Kuwait, December 14-16, 2009; SPE-126410-MS; doi: 10.2118/126410-MS
- Irani, C.; Solubilizing surfactants in miscible drive solvents; U.S. Patent 4,828,029; issued May 9, 1989
- Kuehne, D.L.; Frazier, R.H.; Cantor, J.; Horn Jr., W.; “Evaluation of Surfactants for CO₂ Mobility Control in Dolomite Reservoirs,” SPE/DOE 24177, presented at the SPE/DOE Eighth Symposium on Enhanced Oil Recovery, held in Tulsa, Oklahoma, April 22-24, 1992.
- Le, V.; Nguyen, Q.; Sanders, A.; A novel foam concept with CO₂ dissolved surfactants; presented at the 2008 SPE/DOE Improved Oil Recovery Symposium, Tulsa, OK, April 19-23, 2008; SPE-113370
- Lescure, B.M.; Claridge, E.L.; “CO₂ Foam Flooding Performance vs. Rock Wettability,” SPE 15445, presented at the SPE 61st Annual Technical Conference and Exhibition, held in New Orleans, LA, October 5-8, 1986.
- Romero, L.; Kantzas, A.; “The Effect of Wettability and Pore Geometry on Foamed Gel Blockage Performance in Gas and Water Producing Zones,” SPE 89388, presented at the 2004 SPE/DOE Fourteenth Symposium on Improved Oil Recovery, held in Tulsa, OK, April 17-21, 2004.
- Ryoo, W.; Webber, S.; Johnston, K.; Water in Carbon Dioxide Microemulsions with Methylated Branched Hydrocarbon Surfactants; *Ind. Eng. Chem. Res.* 2003; (42) 6348-6358
- Sanders, A.; Nguyen, Q.; Nguyen, N.; Adkins, S.; Johnston, K.P.; Twin-tailed surfactants for creating CO₂-in-water macroemulsions for sweep enhancement in CO₂ EOR; presented at the Abu Dhabi International Petroleum Exhibition and Conference, held in Abu Dhabi, UAE, November 1-4, 2010; SPE-137689-MS; doi: 10.2118/137689-MS
- Sanders, A.; Successful Implementation of CO₂ Foam for Conformance Control, Dow Oil & Gas, The 4th Annual Wyoming CO₂ Conference, Casper, WY, June 29 and 30, 2010 (oral presentation only)
- Sanders, A.; Jones, R.; Mann, T.; Patton, L.; Linroth, M.; Nguyen, Q.; Successful Implementation of CO₂-Foam for Conformance Control; presentation and slides distributed at the 2010 CO₂ Conference, Midland Texas, December 9-10, 2010.

Schievelbein, V.; Method of decreasing mobility of dense carbon dioxide in subterranean formations; U.S. Patent 5,033,547; issued July 23, 1991

Tan, B.; Cooper, A.; Functional Oligo (vinyl acetate) CO₂-philes for Solubilization and Emulsification; *JACS* 2005; 127(25) 8938-8539

Torino, E.; Reverchon, E.; Johnston, K.P.; Carbon Dioxide/Water, Water/Carbon Dioxide Emulsions and Double Emulsions Stabilized With a Nonionic Biocompatible Surfactant; *J. Colloid Interface Science* 2010; (348) 469-478

Wellington, S.L.; Vinegar, H.J.; Surfactant-Induced Mobility Control for Carbon Dioxide Studied with Computerized Tomography; *Surfactant-Based Mobility Control* 1988; (17) 344-358; *ACS Symposium Series* 1988, (373)

Xing, D.; Wei, B.; McLendon, W.; Enick, R.; McNulty, S.; Trickett, K.; Mohamed, A.; Cummings, S.; Eastoe, J.; Rogers, S.; Crandall, D.; Tennant, B.; McLendon, T.; Romanov, V.; Soong, Y.; CO₂-soluble, Non-ionic, Water-soluble Surfactants that Stabilize CO₂-in-Brine Foams; paper SPE 129907 presented at the 2010 SPE Improved Oil Recovery Symposium held in Tulsa, Oklahoma, USA, 24–28 April 2010

Xing, D.; Wei, B.; McLendon, W.; Enick, R.; McNulty, S.; Trickett, K.; Mohamed, A.; Cummings, S.; Eastoe, J.; Rogers, S.; Crandall, D.; Tennant, B.; McLendon, T.; Romanov, V.; Soong, Y.; CO₂-soluble, Non-ionic, Water-soluble Surfactants that Stabilize CO₂-in-Brine Foams; revised paper SPE 129907 submitted to SPEJ 2011